UNIVERSITA' DEGLI STUDI DI ROMA
"LA SAPIENZA"

ACCADEMIA NAZIONALE DEI LINCEI
ROMA

European Meeting on

"ABSORPTION SPECTROSCOPY IN MINERALOGY"

TUESDAY OCTOBER 4, TO FRIDAY OCTOBER 7, 1988
ROME, ITALY

INVITED LECTURES

DIPARTIMENTO DI SCIENZE DELLA TERRA
Sezione Mineralogico-cristallografica
Università Degli Studi di Roma "La Sapienza"
Piazzale Aldo Moro, 5

INVITED LECTURES

Wednesday, October 5

9.45 - 10.45 J. M. MALEZIEUX (Lille): "*Contribution of the Raman microspectrometry to the study of minerals*".

11.15 - 12.15 J. L. ROBERT (Orléans): "*Relationships between Raman and IR studies in silicates, with special references to layer and chain silicates*".

15.15 - 16.15 D. J. VAUGHAN (Manchester): "*Some contributions of spectral studies in the visible (and near-visible) light region to mineralogy*".

16.45 - 17.45 H. MERIGOUX (Besançon): "*Mineralogical applications of VIS and IR spectroscopy*".

Thursday, October 6

9.00 - 10.00 J. SANZ (Madrid): "*Distribution of the ions in phillosilicates by NMR spectroscopy*".

10.30 - 11.30 A. PUTNIS (Cambridge): "*Combined NMR and vibrational spectroscopic studies of AlSi ordering in minerals*".

11.30 - 12.30 F. SEIFERT (Bayreuth): "*Phase transformations in minerals studied by Mössbauer spectroscopy*".

15.00 - 16.00 K. LANGER (Berlin): "*High pressure spectroscopy*".

16.30 - 17.30 G. CALAS (Paris): "*EXAFS spectroscopy in mineralogy*".

17.30 - 18.30 I. DAVOLI (Camerino): "*Principles and potentials of XANES spectroscopy*".

CONTRIBUTION DE LA MICROSPECTROMETRIE RAMAN A L'ETUDE DES MINERAUX

par J.M. MALEZIEUX

EUROPEAN MEETING

"ABSORPTION SPECTROSCOPY IN MINERALOGY"

Rome - October 4-7 - 1988

INTRODUCTION

C'est par une courte note publiée le 31 Mars 1928 dans la revue "NATURE" (1) que C.V. RAMAN et K.S. KRISHNAN rendirent compte de la découverte de l'effet qui porte le nom du premier nommé.

En s'inspirant des travaux de COMPTON sur la diffusion des R.X. ils supposent qu'il doit exister 2 types de diffusion de la lumière par la matière :

- *"une déterminée par les propriétés optiques des atomes et molécules dans leur état normal",*
- *"une autre représentant les effets des fluctuations de ces atomes et molécules à partir de cet état normal".*

C'est ce second type de diffusion qu'ils mettent en évidence.

Le premier, connu sous le nom de diffusion RAYLEIGH s'effectue sans changement de fréquence et correspond à une diffusion élastique.

L'effet RAMAN, lui, s'accompagne d'un changement de fréquence et correspond à une diffusion inélastique. Cet effet se caractérise par sa faible intensité :

$$10^{-9} < \frac{I_{\text{Raman}}}{I_{\text{Rayleigh}}} < 10^{-6}$$

Si les spectroscopies X ont connu un grand développement en Minéralogie dès les premiers travaux de BRAGG au début du siècle, il n'en est pas de même en ce qui concerne la spectroscopie vibrationnelle RAMAN. La raison est d'ordre méthodologique. En effet, jusqu'à ces dernières années pour obtenir un spectre de diffusion Raman d'un minéral naturel, il fallait disposer d'un monocristal de dimensions suffisantes pour être taillé. Cette condition limitait le champ d'application de la spectroscopie Raman et interdisait toute étude "in situ".

La mise au point il y a une dizaine d'années de la microsonde Raman allait permettre de disposer d'une nouvelle méthode d'analyse en Minéralogie.

Voyons, de façon simplifiée, le principe théorique de la diffusion Raman.

I - PRINCIPE THEORIQUE DE LA DIFFUSION RAMAN.

Un système diffusant soumis à un rayonnement monochromatique de fréquence ν_0 peut diffuser ce rayonnement de 2 façons :

- sans changement de fréquence et c'est la diffusion RAYLEIGH,
- avec un changement de fréquence, et c'est la diffusion RAMAN.

On peut illustrer le processus de diffusion Raman par son diagramme de conservation de l'énergie (Fig. 1).

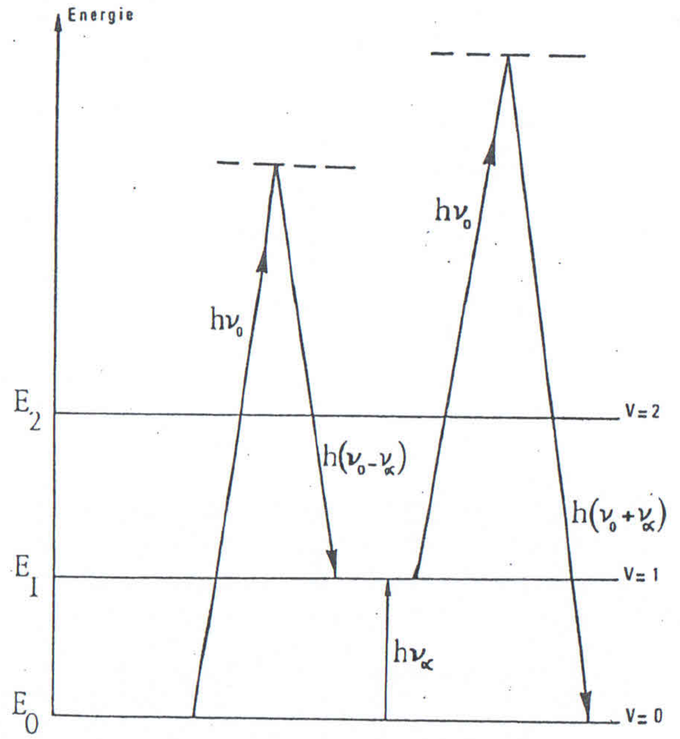

Fig. 1 : DIAGRAMME DE CONSERVATION DE L'ÉNERGIE DANS LE PROCESSUS DE DIFFUSION RAMAN

Si le système diffusant se trouve à un niveau vibrationnel fondamental (ici v = 0) une partie de l'énergie $h\nu_0$ de la radiation incidente est utilisée pour l'amener à un niveau vibrationnel supérieur (ici v = 1). L'énergie du photon diffusé résultant est alors égale à: $h(\nu_0-\nu_\alpha)$.

Si le système diffusant est à un niveau vibrationnel excité, l'énergie du photon diffusé est alors égale à : $h(\nu_0+\nu_\alpha)$.

Au premier cas correspond l'émission d'une raie Raman stokes, au second l'émission d'une raie Raman anti-stokes. Un spectre complet de diffusion Raman contiendra donc des raies stokes et leurs symétriques anti-stokes (Fig. 2).

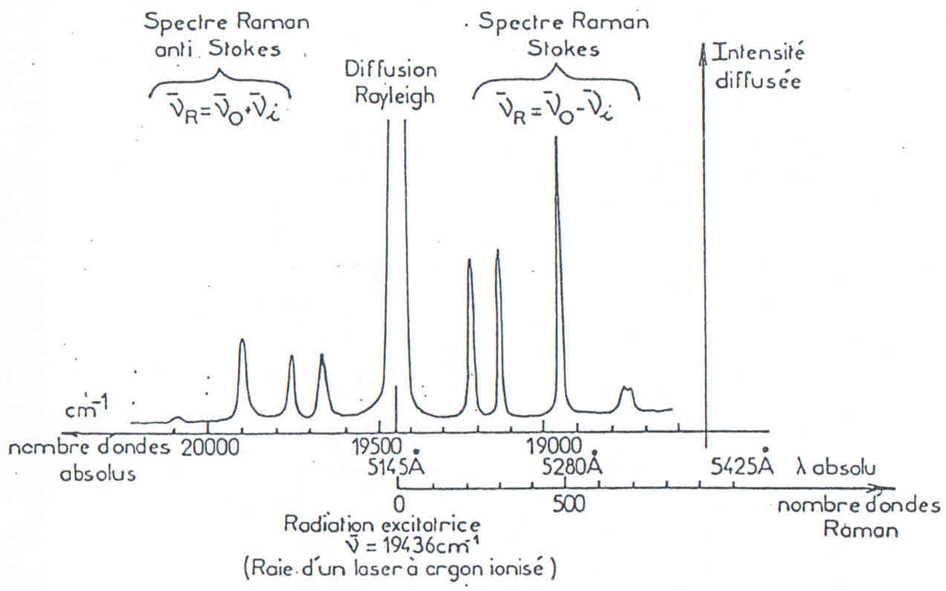

Fig. 2 : Présentation d'un spectre Raman complet (d'après P. DHAMELINCOURT)

Mais les intensités des raies Raman stokes et anti-stokes ne sont pas les mêmes, car elles dépendent avant tout du rapport des populations des niveaux 0 et 1. Le niveau 0 étant beaucoup plus peuplé les raies stokes sont d'intensité beaucoup plus fortes. C'est pourquoi on enregistrera généralement que le spectre Raman stokes.

A chaque $\Delta\nu_i = \nu_0-\nu_i$ correspond un mode de vibration, ν_i étant indépendant de ν_0, et donc une raie Raman. Un calcul théorique, basé sur la théorie des groupes permet de prévoir le nombre de modes de vibration, donc le nombre de bandes, de chaque espèce minérale cristallisée étudiée.

II - INFORMATIONS.

II-a) Informations recueillies :

Elles sont de deux ordres :

- d'ordre structural car les symétries du milieu cristallin étudiées sont en relation avec le nombre de modes de vibration,
- d'ordre chimique car la nature des atomes est en relation avec les fréquences de ces modes.

II-a-1) Information d'ordre structural :

Sans entrer dans le détail des deux méthodes de dénombrement des modes de vibration [méthode de BHAGAVANTAN et VENKATARAYUDU (2) et méthode du site de HALFORD (3)], il faut savoir que puisque toutes les mailles vibrent en phase, il suffit de considérer les opérations de symétrie dans la maille élémentaire ou la maille réduite si la maille élémentaire est multiple. Le nombre N de groupements à considérer est donc égal à :

$$N = \frac{Z}{n}$$

Si Z = nombre de groupements par maille cristallographique

n = multiplicité de cette maille.

Exemple :

Dans la spinelle $MgAl_2O_4$, il y a 8 groupements $MgAl_2O_4$ par maille cristallographique. Celle-ci est cubique face centrée, donc de multiplicité 4. Il y aura donc :

$N = \frac{8}{4} = 2$ groupements $MgAl_2O_4$ dans la maille réduite qui servira à faire le dénombrement des modes de vibration.

Les modes de vibrations se répartissent en modes *internes* et en modes *externes* :

- Les modes *internes* sont constitués par les déformations des molécules (ou des anions complexes dans le cas des cristaux). Ces déformations laissent fixe le centre de masse de ces molécules ou anions complexes,

- les modes *externes* sont constitués par les mouvements d'ensemble de ces entités et se répartissent en :
  - . translations,
  - . et en oscillations de rotations appelés *pivotements* ou *librations*.

II-a-2) Information d'ordre chimique :

La nature des atomes, en l'occurrence leur masse atomique, va être en relation avec la fréquence des modes de vibration. Pour une molécule diatomique la fréquence est proportionnelle à $\sqrt{\frac{k}{\mu}}$ où k est la constante de force et μ la masse réduite.

$$\mu = \frac{M_1 M_2}{M_1 + M_2}$$

D'autre part dans un certain nombre de cas (en particulier celui des solutions solides) la fréquence et/ou l'intensité des bandes seront en relation avec les teneurs en cations substitués.

III - APPAREILLAGE ET METHODOLOGIE.

III-a) Appareillage :

La microsonde Raman (4) encore appelée M.O.L.E. (Molecular Optical Laser Examiner) présente les caractéristiques suivantes (Fig. 3) :

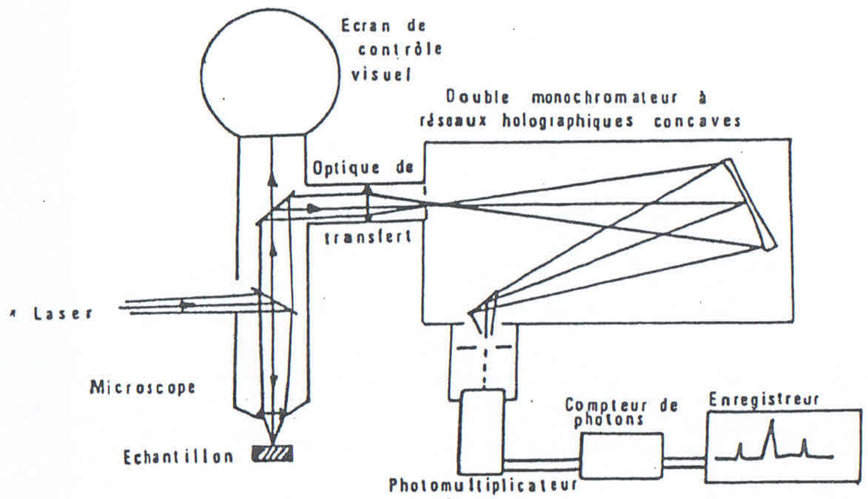

Fig 3 : Schéma simplifié de la microsonde Raman (d'après P. DHAMELINCOURT)

- Le faisceau de lumière monochromatique fourni par un laser est focalisé par un objectif à grande ouverture numérique sur la préparation placée sur la platine d'un microscope. Le même objectif collecte la lumière diffusée qui est analysée par un double monochromateur à réseaux holographiques concaves.

- La détection du signal peut se faire par l'intermédiaire d'un photomultiplicateur suivi d'un compteur de photons (détection monocanal), ou d'une barrette de photodiodes (détection multicanal). Ce dernier mode de détection permet l'exploration instantanée d'un domaine spectral de l'ordre de 500 cm^{-1}.

- L'échantillon peut recevoir soit un éclairement ponctuel, et dans ce cas le volume analysé est de l'ordre du μm^3, soit un éclairement global.

III-b) Méthodologie.

Quels types d'échantillons peut-on étudier ? Puisque le faisceau incident est focalisé par l'intermédiaire de l'objectif d'un microscope, l'objet d'étude peut se présenter sous diverses formes :

- pour les études "in situ" il peut s'agir d'un échantillon brut, d'une lame mince polie, d'une section polie,

- pour les autres études, il peut s'agir d'un monocristal, d'une poudre.

Dans quelles conditions ?

S'il est bien évident que toutes les études à T et P ambiantes sont possibles, on peut aussi faire des études à température variable en couplant à la microsonde une platine chauffante ou réfrigérante. Il est de même possible de faire des études à haute pression en couplant à la microsonde une cellule appropriée. Nous en verrons des exemples dans la suite de cet exposé.

IV) PROBLEMES SUSCEPTIBLES D'ETRE ETUDIES.

Ces problèmes sont de nature diverse. A l'heure actuelle les différentes études minéralogiques en microspectrométrie Raman concernent les thèmes suivants :

IV-a) Identification d'espèces minérales :

Un spectre de diffusion Raman, au même titre qu'un diffractogramme X, est une "carte d'identité" de l'objet diffusant. Des microphases dont la largeur ne dépasse pas quelques microns peuvent donc être identi-

fiées. Le faisceau incident pouvant être focalisé à l'intérieur de la préparation il est aussi possible d'identifier des inclusions, fluides ou solides. En ce qui concerne les inclusions fluides, la microspectrométrie Raman est la seule méthode d'analyse qualitative non destructive.

IV-b) Comportement vibrationnel des solutions solides :

La réponse spectrale dépendant de la composition chimique de l'échantillon, les substitutions qui entrent en jeu auront dans la plupart des cas une influence sur les caractéristiques des spectres obtenus pour diverses compositions chimiques.

D'une façon générale, et sur la base d'une substitution bicationique, deux types de comportement vibrationnels sont susceptibles de se produire (5) :

- Si les cations qui se substituent sont de nature chimique et de masses très voisines, les mouvements de ces cations sont alors très fortement couplés et les *fréquences* des modes évoluent de façon quasi linéaire entre les pôles de la série. C'est ce que l'on appelle un comportement vibrationnel à *1 mode*.

- Dans le cas où les deux cations qui se substituent ont des masses très différentes, les deux types de modes imposés par chacun de ces cations coexistent. *L'intensité* des modes correspondant à chaque cation dépend de la teneur de ce dernier dans la solution solide et évolue entre les deux pôles de la série. C'est ce que l'on appelle un comportement vibrationnel à *2 modes*.

Entre ces deux types de comportements extrêmes peuvent exister des comportements vibrationnels "intermédiaires", c'est-à-dire que des solutions solides peuvent donner des spectres Raman dans lesquels certains modes évoluent dans un comportement à *1 mode* et d'autres dans un comportement à *2 modes*.

IV-c) Etudes en fonction de T et P :

IV-c-1) Transitions de phase :

Les transformations polymorphiques qui se produisent soit en fonction de la température (ex. aragonite——>calcite), soit en fonction de la pression (ex. Calcite I——>Calcite II——>Calcite III) peuvent être suivies par spectrométrie Raman. Les symétries du milieu diffusant étant un des facteurs prépondérants, toutes modifications de ces symétries auront pour conséquence de modifier les spectres de diffusion Raman des milieux polymorphes.

IV-c-2) Accès à certains paramètres thermodynamiques :

Les variations de température et de pression induisent des variations de volume du solide cristallin étudié, et ces variations de volume font influer sur les fréquences des modes de vibration des liaisons. Ces effets de la température et de la pression peuvent être estimés expérimentalement par l'obtention des paramètres de GRUNEISEN (6-7).

Ce paramètre γ_i a pour formule générale :

$$\gamma_i = - \partial \ln \nu_i / \partial \ln V$$

La variation de volume dépendra soit de la variation de température, soit de la variation de pression. Il s'en suit que l'on peut définir deux paramètres de GRUNEISEN tenant compte de ces deux facteurs :

$\gamma_{i,P}$ à T cste.

$\gamma_{i,T}$ à P cste.

Ces deux paramètres s'écrivent comme suit :

$$\gamma_{i,P} = \frac{K_T}{\nu_i} \frac{\partial \nu_i}{\partial P}$$

$$\gamma_{i,T} = \frac{1}{\alpha \nu_i} \frac{\partial \nu_i}{\partial T}$$

où K = module d'incompressibilité, tabulé pour diverses espèces minérales.

α = coefficient de dilatation thermique.

$\frac{\delta \nu_i}{\delta P}$ et $\frac{\delta \nu_i}{\delta T}$ sont les pentes des droites corrélant les glissements de fréquences ν_i de chaque mode en fonction de P et T.

Les différences $\gamma_{i,T} - \gamma_{i,P}$ seront une mesure des contributions harmoniques ou anharmoniques des liaisons du cristal dans l'expression de son énergie interne U.

La liste des problèmes minéralogiques susceptibles d'être abordés par le biais de la microspectrométrie Raman, qui est exposée ci-dessus, n'est bien sûr pas exhaustive, mais correspond aux divers axes de recherches développés à l'heure actuelle en France.

V - EXEMPLES.

V-a) Identification d'espèces minérales et d'inclusions fluides :

V-a-1) Espèces minérales :

Il existe à l'heure actuelle un grand nombre d'espèces minérales pour lesquelles sont connus les spectres de diffusion Raman. Les minéraux qui se présentent couramment sous forme de monocristaux (quartz, carbonates) ont été les premiers à fournir des spectres en diffusion Raman classique.

L'exemple présenté ici concerne un problème d'identification de microphases. Il s'agit de la mise en évidence de lamelles de grenat in-

incluses dans du clinopyroxène à la suite d'expériences de réhomogénéisation sous haute pression et haute teméprature. La difficulté de l'identification résidait dans le fait que les zones de grenat et/ou de pyroxène avaient des largeurs de l'ordre de quelques microns.

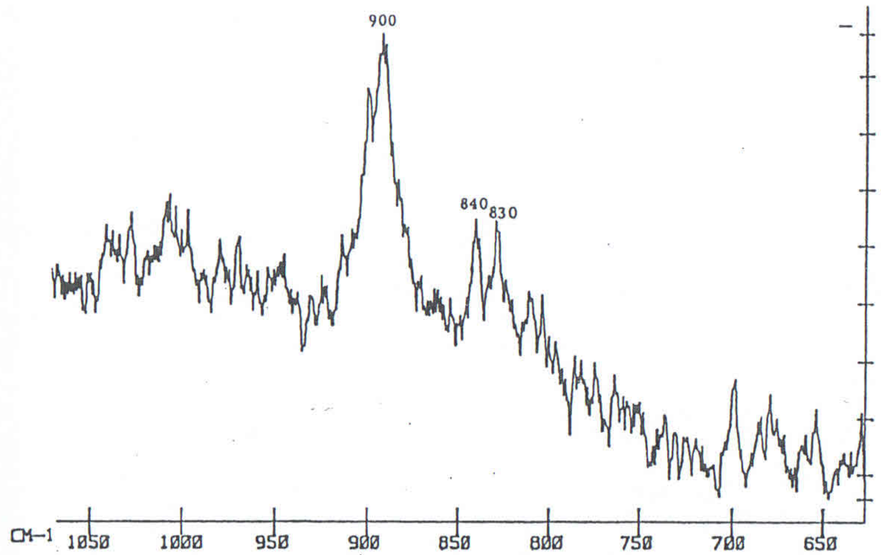

Fig. 4b - Characteristic Raman bands of garnet

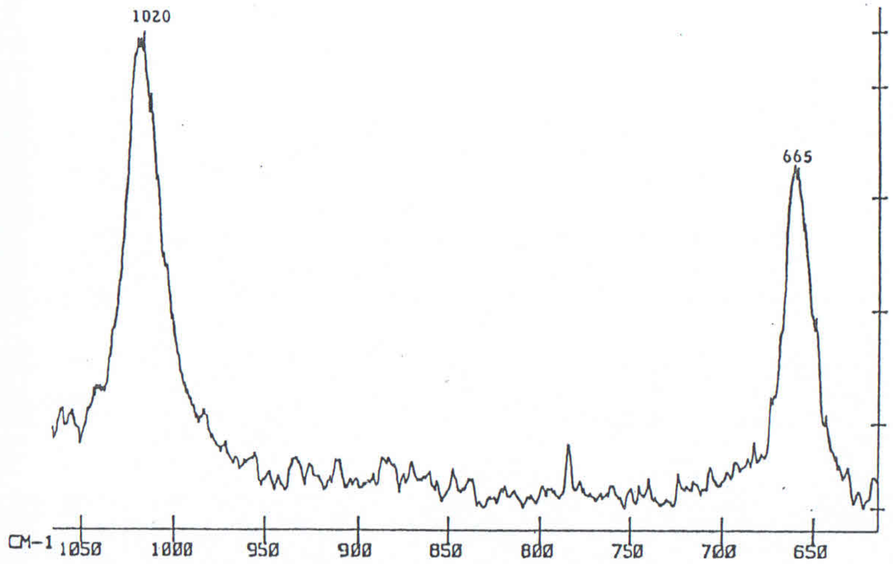

Fig. 4a - Characteristic Raman bands of clinopyroxène

Les spectres présentés sur la figure 4a-4b permettent d'identifier sans ambiguïté une phase de clinopyroxène (proche du diopside) par ses raies à 665 et 1020 cm^{-1} et une phase de grenat (proche du pyrope) par ses raies à 830, 840 et 900 cm^{-1}.

V-a-2) Inclusions fluides :

La microsonde Raman permet l'identification d'inclusions fluides monophasées ou multiphasées. A partir des sections efficaces de diffusion Raman relatives et de la courbe de réponse spectrale de l'instrument on peut déterminer les fractions molaires des constituants d'un mélange (8).

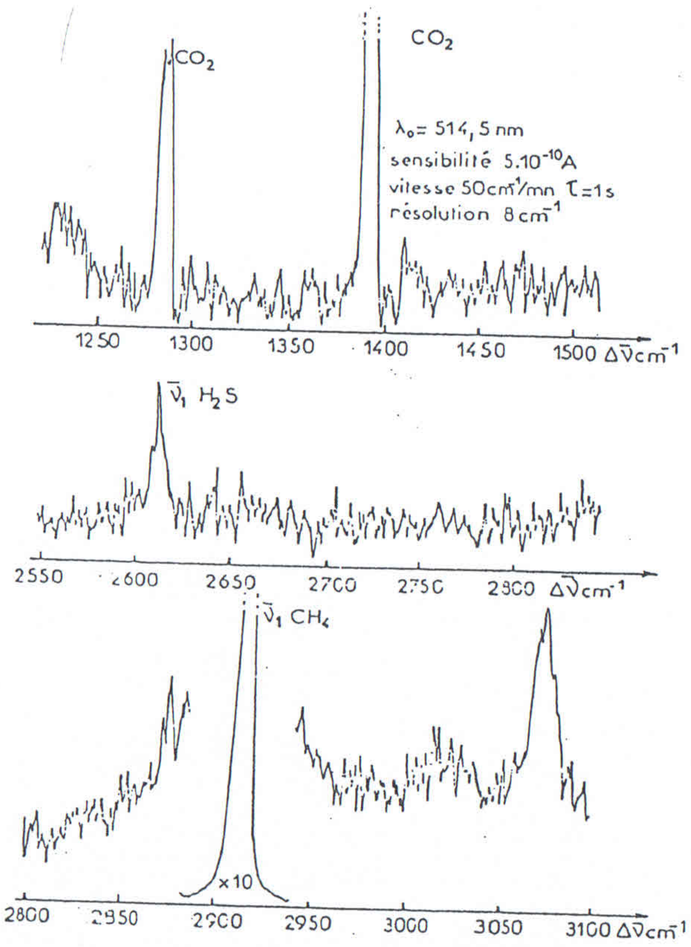

Fig. 5 : *Analyse d'une inclusion monophasée dans un quartz provenant des Dolomies de Lastourville (Gabon).* (D'après P. DHAMELIN - COURT - Thèse - LILLE).

La figure 5 montre les résultats obtenus lors de l'analyse d'une inclusion monophasée contenue dans un quartz provenant des Dolomies de Lastourville (Gabon).

Cette inclusion gazeuse est essentiellement constituée de CH_4, CO_2 et H_2S avec des fractions molaires respectives de 66%, 33% et 1%.

Il est de même possible d'effectuer des analyses dans des inclusions fluides multiphasées.

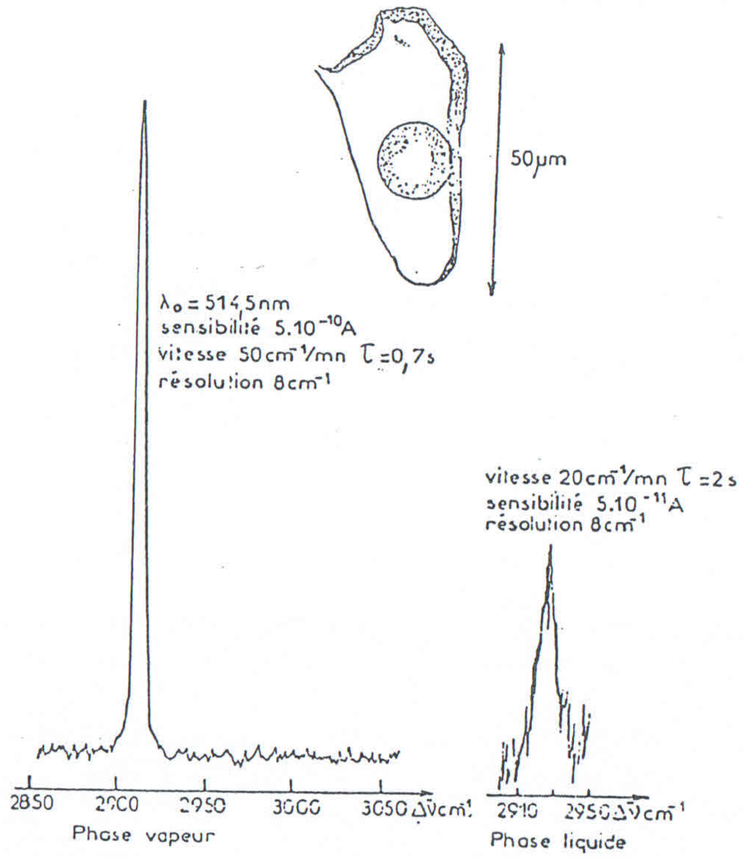

Fig. 6 : *Analyse d'une inclusion biphasée $CH_4(v)$ - $H_2O(\ell)$ dans un quartz provenant de Vermuthgluh (Suisse).* (D'après P. DHAMELINCOURT - Thèse - LILLE).

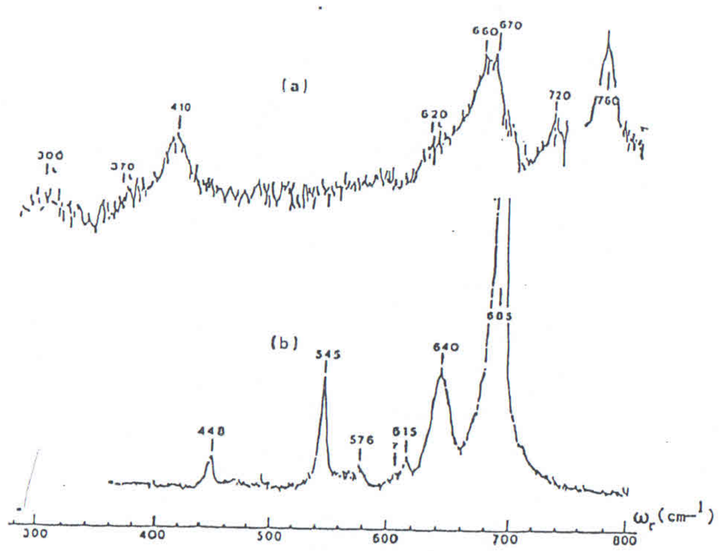

Fig. 7 : Spectres Raman de deux termes de la série $MgAl_{2-x}Cr_xO_4$. (a) : x = 0,12 ; (b) : x = 1,98

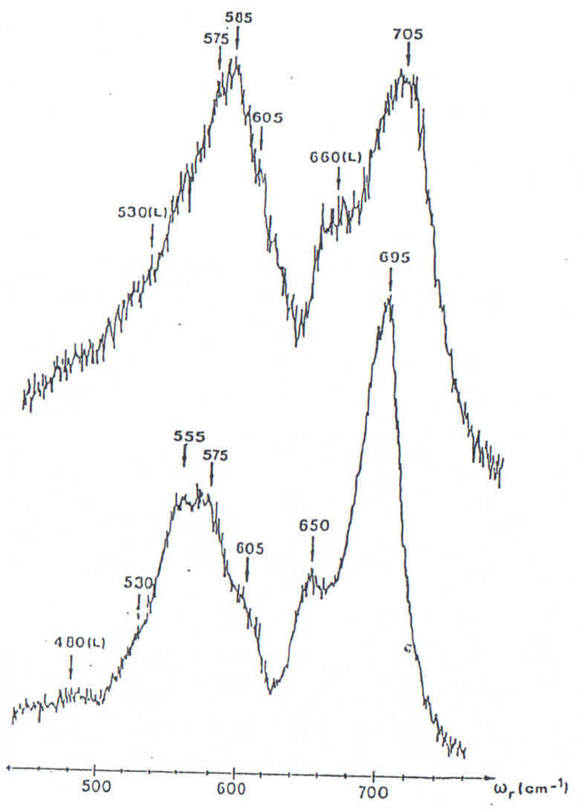

Fig. 8 : Spectres Raman de deux chromites naturelles.

Les spectres présentés sur la figure 6 correspondent à ceux d'une inclusion fluide biphasée (gaz + liquide) dans un quartz. Le méthane détecté correspond à une teneur très faible (quelques ppM).

On peut d'autre part mesurer la pression dans l'inclusion par le décalage en fréquence, due à cette pression, de la raie du méthane dissous dans H_2O (Fig. 6).

V-b) Comportement vibrationnel de solutions solides : exemple des spinelles :

L'exemple choisi concerne les chromites associées à des roches ultrabasiques (péridotites et pyroxénolites) appartenant à divers complexes ophiolitiques.

La formule générale des chromites :

$$(Mg, Fe^{2+})\ (Cr, Al, Fe^{3+})_2O_4$$

montre que deux types de substitutions sont possibles. Il s'agit des substitutions entre cations bivalents et de celles entre cations trivalents. Il était donc a priori difficile de pouvoir interpréter des variations enregistrées dans les spectres Raman de ces composés. Il s'est donc avéré nécessaire d'obtenir en premier lieu des spectres sur des composés plus simples ne mettant en jeu qu'un type de substitution. Ces composés synthétiques appartiennent aux séries suivantes : $MgAl_{2-x}Cr_xO_4$, $FeAl_{2-x}Cr_xO_4$, $Mg_{1-x}Fe_xAl_2O_4$, $Mg_{1-x}Fe_xCr_2O_4$. Des termes de la série $Mg_{1-\frac{x}{2}}Fe_{\frac{x}{2}}Al_{2-x}Cr_xO_4$ proche par leur composition des chromites naturelles ont aussi été synthétisés.

Sans entrer dans le détail de cette étude (9-10) il apparaît (Fig. 7) que les spinelles de synthèse peuvent présenter, simultanément ou non, deux types de comportements vibrationnels :

- un comportement à "1 mode" qui se traduit par un glissement de fréquence de la bande de plus haute fréquence,

- un comportement à "2 modes" se traduisant par l'apparition de bandes de basses fréquences en-dessous de 450 cm^{-1}.

Les chromites naturelles présentent des spectres de diffusion Raman dans lesquels seul le comportement à "1 mode" a lieu (Fig. 8).

Ce comportement à "1 mode" est essentiellement dû aux substitutions intéressant les cations trivalents. Il a donc été possible de corréler la variation de fréquence de la bande de plus haute fréquence (mode A_{1g}) avec le rapport $(Cr + Fe^{3+})/(Cr + Al + Fe^{3+})$ et d'obtenir ainsi un moyen rapide d'analyse des chromites naturelles au regard de la classification proposée par STEVENS (Fig. 9).

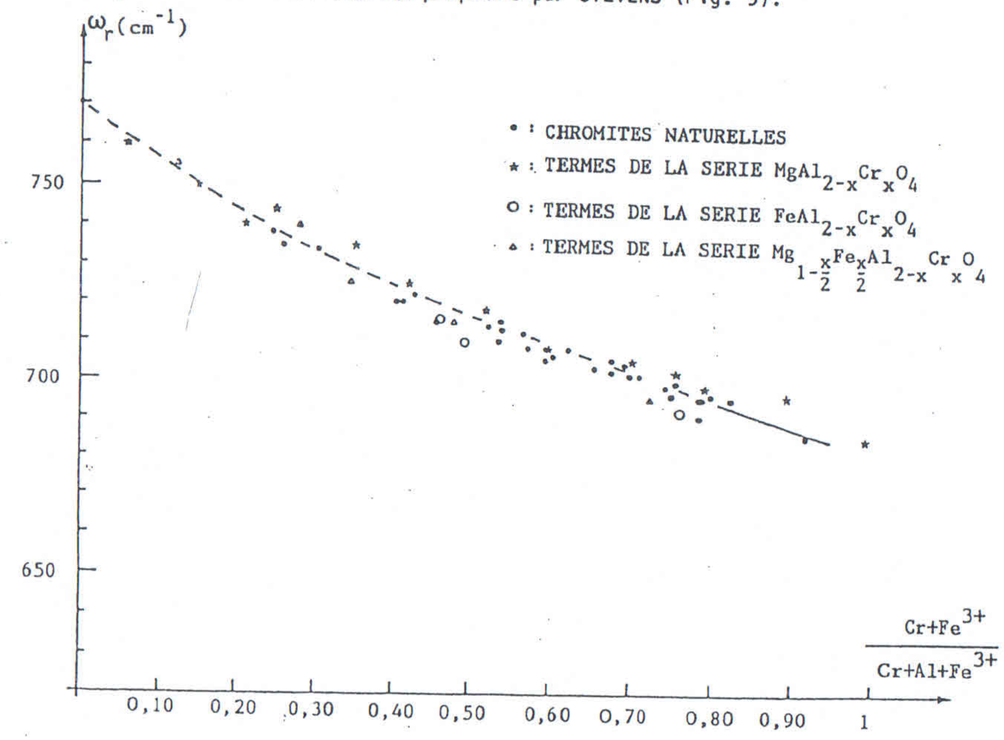

Fig. 9 : Corrélation entre la fréquence du mode A_{1g} et le rapport $(Cr + Fe^{3+})/(Cr + Al + Fe^{3+})$ dans les chromites naturelles et les composés des séries synthétiques.

V-c) Etudes en fonction de T et P.

V-c-1) Transition de phase :

- *En fonction de T :*

L'exemple choisi est celui de la transition aragonite ⟶ calcite au-dessus de 400°C. Cette transition de phase (passage d'une structure orthorhombique à une structure rhomboédrique) introduit de grandes modifications dans les spectres de diffusion Raman de ces deux composés (Fig. 10).

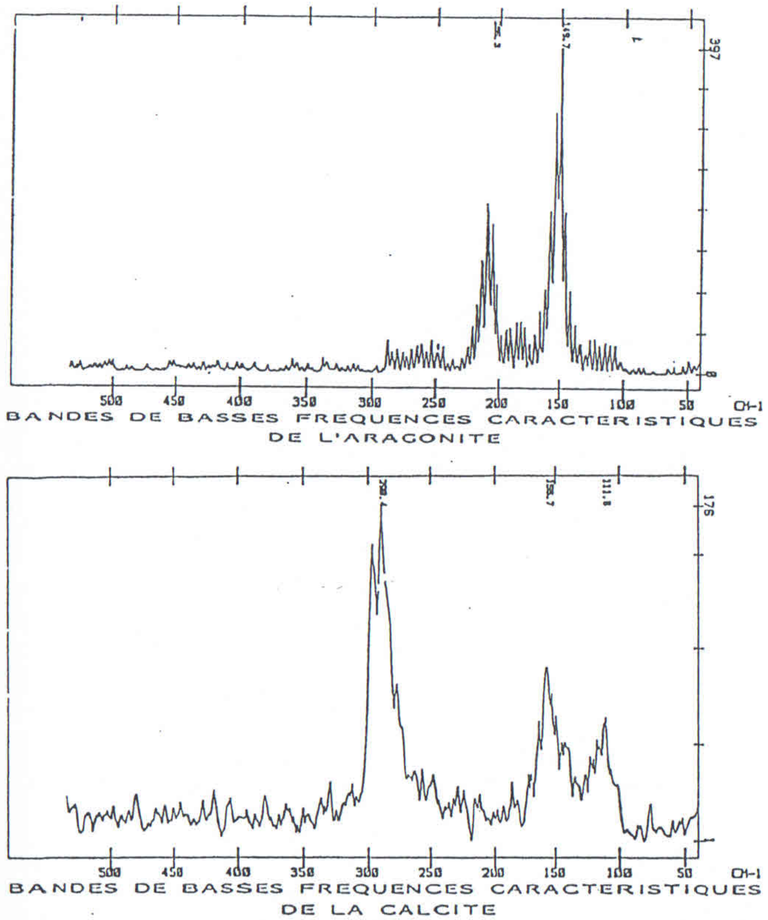

Fig. 10 : Mise en évidence de la transition de phase Aragonite⟶ Calcite (T >400°C) par leurs spectres Raman de basse fréquence.

Expérimentalement, ces spectres sont obtenus en couplant à la microsonde une platine chauffante (type Leitz). La transition aragonite⟶ calcite s'observe particulièrement dans le domaine des basses fréquences. La raie à 206 cm^{-1} caractéristique de l'aragonite disparaît au-dessus de 400°C et la raie à 290 cm^{-1} caractéristique de la forme calcite apparaît.

- *En fonction de P :*

L'exemple choisi concerne divers polymorphes de la calcite en fonction de la pression : Calcite I (ou P ambiante), Calcite II (à P ≥ à 14 Kbar) et Calcite III (à P ≥ à 19 Kbar).

Les spectres ont été obtenus en couplant à la microsonde une cellule à enclumes de saphir. Le calcul de la pression se fait à partir des transitions de phases, optiquement visibles, des deux constituants du milieu de confinement (RbCL + KBr) (Fig. 11).

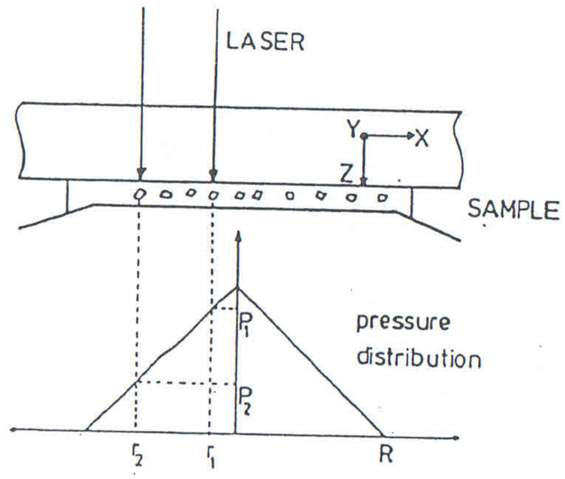

Fig. 11 : L'échantillon comprimé entre les 2 saphirs est constitué d'un mélange de RbCl, KBr et de particules de calcite. La pression augmente continûment du bord vers le centre. Il est donc possible d'étudier des particules minérales à différentes pressions en focalisant le laser sur celles-ci par l'intermédiaire d'une table micrométrique fixée à la cellule.

Des spectres Raman de $CaCo_3$ à différentes pressions (c'est-à-dire dans des localisations différentes dans la cellule) sont présentés figure 12. Le spectre Raman de la calcite à pression ambiante (Calcite I) montre les cinq bandes caractéristiques et leurs fréquences correspondent bien à celles obtenues par PORTO *et al.* (11) par la méthode classique. La bande à 750 cm^{-1} est une bande du saphir.

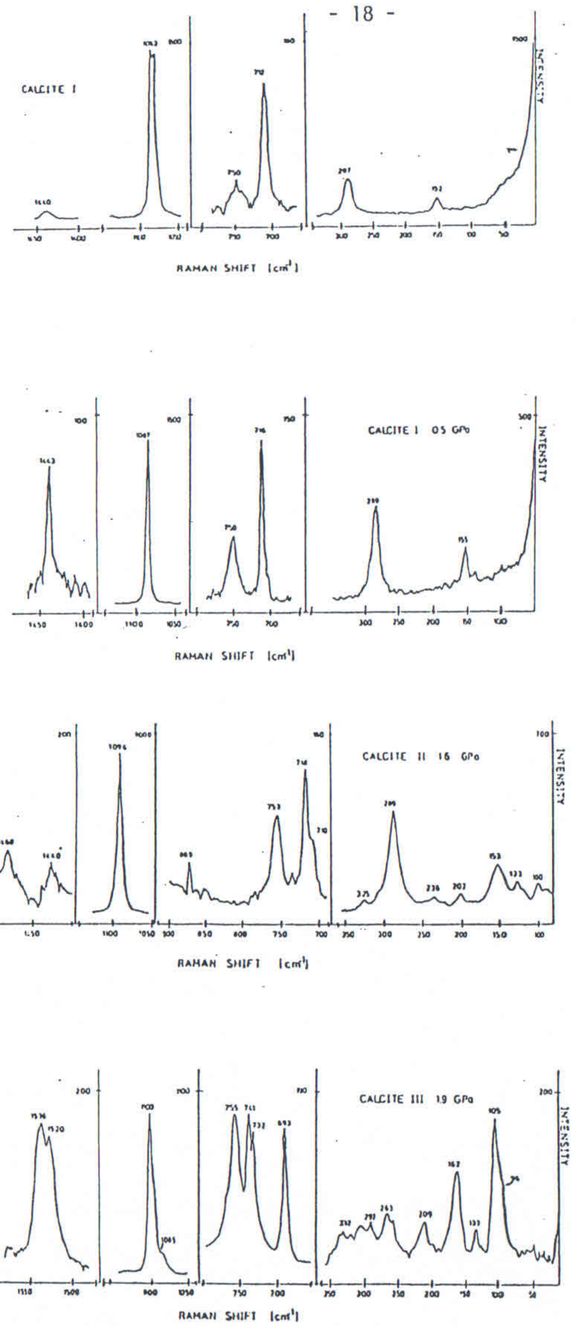

Fig. 12 : Spectres Raman du carbonate de calcium obtenus en cellule saphir.

Le spectre obtenu à la pression de 0,5 GPa (= 5 Kbar) est presque similaire à celui obtenu à pression ambiante. On observe une augmentation des fréquences avec la pression, résultats cohérents avec ceux présentés par FONG et NICOL (12).

Les spectres de la Calcite II et de la Calcite III sont aussi cohérents avec ceux des auteurs cités dessus. La raie à 869 cm^{-1} dans le spectre de la Calcite II correspond à un mode ν_2 (déformation hors du plan dans CO_3^{--}) et suggère une perte de centre de symétrie pour cette phase.

Il faut signaler que l'utilisation d'une telle cellule couplée à une microsonde à détection multicanal permet d'obtenir rapidement (temps total de l'ordre de 10 minutes) des spectres correspondant à différentes pressions comprises entre 0 et 25 Kbar).

V-c-2) Accès à certains paramètres thermodynamiques : l'exemple de $Ca_2 Ge O_4$:

Les contributions anharmoniques à l'équation d'état des solides minéraux du manteau représentent l'un des problèmes de la minéralogie et de la géophysique actuelles, susceptible d'être abordé par le biais de la microspectrométrie Raman.

Cette anharmonicité est responsable de propriétés telles que :

- l'expansion thermique,
- les décalages en fréquence des modes normaux de vibration avec la température ou la pression.

Cet effet de la pression et de la température sur les fréquences de vibrations d'une liaison peut être estimé expérimentalement par l'obtention des paramètres de GRUNEISEN (cf. § IV-c-2).

C'est ce qui a été fait sur $Ca_2 Ge O_4$, un isotype de Mg_2SiO_4. Les spectres ont été enregistrés entre 0 et 1 000 cm^{-1} en fonction de la température jusqu'à 1 000°C et en fonction de la pression entre 10^5 Pa et 3 GPa. Les techniques utilisées dans ces deux types d'expériences sont celles précédemment décrites.

Les pentes des droites qui corrèlent les variations de fréquences de chaque mode en fonction de T et P permettent de calculer les $\gamma_{i,T}$ et $\gamma_{i,P}$ associés à ces modes.

Ces valeurs sont présentées sur le tableau ci-dessous.

fréquence (cm^{-1})	$\gamma_i P$	$\gamma_i T$	
757	0.74	0.83	élongation liaisons Ge — O
732	0.61	0.75	
697	0.48	0.65	
682	0.62	0.61	
663	0.59	0.72	
464	1.09	0.37	déformations et torsions Ge — O Ca — O
445	1.20	1.00	
415	1.09		
362	1.25	1.36	
353	1.44	1.16	
302	2.52	1.60	
286		1.99	
263	1.61	0.90	
250	1.92		
222	1.91	1.58	
140	1.41	0.00	

Paramètres de GRUNEISEN des 16 modes observés dans Ca_2GeO_4.

Les modes de hautes fréquences (> 500 cm^{-1}) sont relatifs aux modes internes des entités GeO_4 et correspondent aux élongations Ge-O.

Les modes de basses fréquences groupent les déformations et torsions Ge-O, Ca-O ainsi que les translations d'ensembles des groupements GeO_4 et des ions Ca. Ce sont les modes externes de vibration.

A la lecture du tableau on remarque que les $\gamma_{i,T}$ et $\gamma_{i,P}$ des modes de basses fréquences sont supérieurs à ceux des modes de hautes fréquences. Ceci s'explique par le fait que pour un mode donné :

- $\gamma_{i,P}$ varie comme $K_T d^3$, d étant la longueur des liaisons. Or, les modes de hautes fréquences sont relatifs aux vibrations des liaisons Ge-O dans GeO_4 dont la longueur est de l'ordre de 1,7 Å. Les modes externes de basses fréquences impliquent des mouvements d'ensemble des entités GeO_4 dont les distances mutuelles sont supérieures à 2 Å, les distances Ca-O étant aussi supérieures à 1,7 Å.

- $\gamma_{i,T}$ varie comme $\frac{\alpha_i}{\alpha}$, α_i étant le coefficient de dilatation de la liaison considérée et α le coefficient de dilatation macroscopique. Pour les modes de hautes fréquences α_i est petit car Ge a une coordinance faible et un nombre de charges élevé.

Les différences $\gamma_{i,T} - \gamma_{i,P}$ permettent de mesurer les contributions harmoniques ou anharmoniques de liaisons impliquées dans chaque mode de vibration :

Si $\gamma_{i,T} - \gamma_{i,P} = 0$ la contribution est harmonique,

Si $\gamma_{i,T} - \gamma_{i,P} \neq 0$ elle est anharmonique.

Ces différences pour les modes de hautes fréquences sont faibles, voire nulles, mais importantes pour les modes de basses fréquences.

Il s'en suit que les vibrations correspondant aux modes internes des groupements GeO_4 ont un comportement harmonique ou quasi-harmonique.

La contribution anharmonique provient des liaisons Ca-O correspondant à certains des modes de basses fréquences.

VI - CONCLUSIONS.

A travers ces divers exemples, il apparaît que la microspectrométrie Raman doit être considérée comme une nouvelle méthode d'investigation en Minéralogie. Combinant les avantages d'une analyse non-destructive et in situ, elle vient utilement compléter la panoplie des méthodes habituellement utilisées. Mais il est bien sûr évident, qu'en fonction des problèmes étudiés, elle ne saurait répondre à toutes les questions. Son grand mérite est de permettre de faire entrer la spectrométrie vibrationnelle dans des domaines qu'elle avait jusqu'à présent peu ou pas explorés.

BIBLIOGRAPHIE

(1) C.V. RAMAN and K.S. KRISHNAN : "A new type of secondary radiation" *Nature*, 121, p. 501, (1928).

(2) S. BHAGAVANTAM, T. VENKATARAYUDU : "Theory of groups and its application to physical problems" - Bangalore Press - Bangalore City, INDIA and al., (1951).

(3) R.S. HALFORD : "Motions of molecules in condensed systems : I Selections rule, relative intensities and orientations effects for Raman and infraned spectra" - *J. Chem. Phys.*, 14, p. 8-15, (1946).

(4) P. DHAMELINCOURT : "Etude et réalisation d'une microsonde moléculaire à effet Raman. Quelques domaines d'application" - *Thèse*, Université de Lille I, (1979).

(5) A.S. BARKER Jr., A.J. SIEVERS : "Optical studies of the vibrational properties of disorded solid" - *Review of Modern Physics*, 47, suppl. n° 2, p. S3-S168, (1975).

(6) T.H.K. BARRON : "Gruneisen parameters for the equation of state of solids" - *Ann. Phys.*, 1, p. 77-90, (1957).

(7) S.W. KIEFFER : "Thermodynamics and Lattice vibrations of minerals : 5. Applications to phase equilibra, isotopic fractionation, and high-pressure thermodynamic properties" - *Rev. Geophys. Space Phys.*, 20, n° 4, p. 827-849, (1982).

(8) P. DHAMELINÇOURT, J.M. BENY, J. DUBESSY : "Analyse d'inclusions fluides à la microsonde MOLE à effet Raman" - *Bull. Minéral.*, 102, p. 600-610, (1979).

(9) J.M. MALEZIEUX : "Contribution à l'étude de spinelles de synthèse et de chromites naturelles par microsonde Raman Laser" - *Thèse*, Université de Lille I, (1985).

(10) J.M. MALEZIEUX et B. PIRIOU : "Relation entre la composition chimique et le comportement vibrationnel de spinelles de synthèse et de chromites naturelles en microspectrométrie Raman" - *Bull. Minéral.*, (à paraître).

(11) S.P.S. PORTO, J.A. GIORDMAINE, T.C. DAREN : "Depolarization of Raman scattering in calcite" - *Phys. Rev.*, 147, p. 608-611, (1966).

(12) M.J. FONG and M. NICOL : "Raman spectra of calcium carbonate at high-pressures" - *J. Chem. Phys.*, 54, p. 579-587, (1971).

OUVRAGES GENERAUX

J. BARRIOL, J.L. RIVAIL : "Spectroscopie de la molécule" - Collection S.U.P., P.U.F. (1970).

F.A. COTTON : "Application de la théorie des groupes à la Chimie"- Dunod Editeur (1968).

W.G. FATELEY, F.A. DOLLISH, M.T. McDEVITT, F.F. BENTLEY : "Infrared and Raman selection rules for molecular and lattice vibrations : The correlation method" - Wiley Interscience, John Wiley and Sons, Inc. (1972).

G. HERZBERG : "Molecular spectra and molecular structure. II. Infrared and Raman spectra of polyatomic molecules" - Van Nostrand Reinhold Company (1945).

Th. KAHAN : "Théorie des groupes en physique classique et quantique". Tome 2 : "Applications en physique classique" - Dunod Editeur (1971).

H. POULET, J.P. MATHIEU : "Spectres de vibration et symétrie des cristaux" - Gordon and Breach, Science Publishers, Inc. (1970).

G. TURREL : "Infrared and Raman spectra of crystals" - Academic Press (1972).

RELATIONSHIPS BETWEEN RAMAN AND IR STUDIES IN SILICATES, WITH SPECIAL REFERENCE TO LAYER AND CHAIN SILICATES.

Jean-Louis ROBERT G.S. C.N.R.S.-B.R.G.M., 1A, rue de la Férollerie
45071 ORLEANS Cedex 2, FRANCE

Though Raman and infrared (IR) absorption concern two different aspects of vibrational spectrometries, these two approches provide similar or complementary structural informations. This lecture deals with the fundamental features that can be derived from Raman and IR spectra of layer silicates, micas essentially and smectites, and chain silicates amphiboles. The emphasis is put on the similarities between these two mineralogical families.

Four wavenumber ranges are distinguished: the high-wavenumber range (3500 cm^{-1} and above), typical of OH-stretching vibrations; the domain of Si-O valence vibrations (around 1000 cm^{-1}); the domain of Si-O-Si (and Si-O-Al) stretching vibrations(700-600 cm^{-1}) and ,briefly,the complex low wave number range, below 600 cm^{-1}.

The high-wavenumber range: 3800 - 3500 cm^{-1}.

The main structural features of layer silicates (micas and smectites) and chain silicates (amphiboles) around an OH group can be deived from OH-stretching wavenumbers. These wavenumbers, measured by IR absorption and Raman scattering spectrometries, are equal within experimental errors, in natural as well as synthetic silicates, indicating that the in-phase and out-of-phase OH vibrations have the same wavenumbers, with little coupling (or no) between them.

Micas and smectites.

Determination of the site occupancy of the three octahedrally coordinated positions adjacent to the hydroxyl group: distinction between trioctahedral environments (formally high wavenumbers, superior to ≈ 3650 cm^{-1}) and dioctahedral ones (< 3650 cm^{-1}), in layer silicates free of transition elements.

Identification of the sum of cationic charges adjacent to the OH group and demonstration of the existence of a limited set of possible cationic arrangements (5 charges: M^{2+}_2Li and Li_2M^{3+}, 6 charges: M^{2+}_3 and $M^{3+}M^{2+}Li$, 7 charges: $M^{2+}_2M^{3+}$ and M^{3+}_2Li, 8 charges: M^{2+}_2Ti).

Systematic decrease of OH-stretching wavenumbers with increasing the bulk Al content, for each type of OH group observed in trioctahedral phases and opposite behaviour of OH-stretching wavenumbers in dioctahedral phases. Four equations are sufficient to account for these variations in Li, Mg, Al phases:

a) $\nu = -9.33\ Al + 3754$ (5-charge environments)

b) $\nu = -16.95\ Al + 3741$ (6-charge environments)

c) $\nu = -29.66\ Al + 3719$ (7-charge environments); a), b), and c) are for trioctahedral phases;

d) $\nu = +11.45\ Al + 3592$ in the dioctahedral family. The OH-stretching wavenumbers are given in cm^{-1}. A value is available for the 8-charge environment Mg_2Ti, observed in the synthetic mica $Na(Mg_{2.75}Ti_{0.25})(Si_{2.5}Al_{1.5})O_{10}(OH)_2$; this value , 3640 cm^{-1}, is in line with equations a), b), and c).

A similar behaviour is observed in 2 : 1 layer silicates containing transition elements, only slopes and ordinates at the origin are different. This is observed for example on the join annite - siderophyllite or its nickeliferous and cobaltiferous equivalents. These variations are controlled by OH...O interactions between the hydroxyl proton and the apical oxygens of tetrahedra.

Evidence for tetrahedrally coordinated divalent cations (Be, Mg, Co, Ni), responsible for very low OH-stretching wavenumbers, e.g., 3507 cm^{-1} in a synthetic low-Al mica having 0.375 $(Ni^{2+})^{IV}$ per formula unit, based on 11 oxygens.

Identification of the nature of the interlayer cation (or absence of a cation); for example, the replacement of K^+ by Ba^{2+} increases the wavenumber by about 30 cm^{-1}. The state of hydration of the alkali-cation of smectites can also be determined by the presence of "talc-like" wavenumbers, at about 3680 cm^{-1}, in the spectra of hydrate-I (2 H_2O) and hydrate-II (5 H_2O).

Order-disorder relationships in tetrahedral as well as octahedral layers, e.g., exclusion of Al^{IV} and Li^{VI} from the vicinity of an octahedral vacancy.

Amphiboles.

Structural informations provided by the OH-stretching region of amphiboles are essentially similar to that obtained on micas.

Distinction between amphiboles with a free (or partially free) A-site, characterized by a "tremolite-type" band, around 3670 cm^{-1} (3663 cm^{-1} in glaucophane, 3670 cm^{-1} in gedrite, 3668 cm^{-1} in anthophyllite, 3672 cm^{-1} in actinolite), and amphiboles which exhibit a high-wavenumber OH band, due to hydroxyls pointing towards an occupied A-position (3730 cm^{-1} in Na-richterite, 3720 cm^{-1} in pargasite).

Evidence for the positional disorder of the A-cation over the A(2/m) and A(m) subsites in K-richterites, by the splitting of the OH-stretching band into two components, at 3730 and 3735 cm^{-1}, respectively.

Distribution of Mg^{2+} and Fe^{2+} over M(1) and M(3) sites. This topic is abundantly documented in literature and will not be considered here.

Evidence for the distribution of high-charge cations (Al^{3+}, Ti^{4+}) over M(2), M(1) and M(3) sites; e.g., presence of a major intensity band at 3686 cm^{-1}, typical of a 7-charge environment (Mg_2Al) in synthetic pargasite.

The domain of Si-O valence vibrations.

In micas and smectites, the salient feature observed in this range is the presence of a high-wavenumber medium-intensity band (1100 cm^{-1} and above), in the IR spectra of tetrasilicic micas (tetrasilicic magnesium mica :$KMg_{2.5}Si_4O_{10}(OH)_2$, taeniolite : $K(Mg_2Li)Si_4O_{10}(OH)_2$, and solid solutions involving polylithionite : $K(Li_2Al)Si_4O_{10}(OH)_2$ as a major component); this high-wavenumber band corresponds to the A1 and B1 stretching modes; it is systematically observed in micas with a very short T - O(3) bond length - O(3) is the apical oxygen - for example, 1.564 Å in polylithionite. A second band Si-O stretching band is typical of tetrasilicic compositions; it occurs at wavenumbers around 960 cm^{-1}, with a high intensity and correspond to the E1 mode; it reflects long $Si\text{-}O_{bridging}$ bond lengths. With increasing Al^{IV} content, new bands are generated between these two extreme wavenumber values; they indicate the progressive evolution of the flattened tetrahedron (symmetry C_{3v}) towards a more regular geometry (symmetry T_d). This is observed on the joins tetrasilicic magnesium mica - phlogopite, polylithionite - phlogopite and taeniolite - phlogopite. Raman scattering offers much less informations in this wavenumber range; only one single low-intensity high-wavenumber band is observed in most cases, around 1140 cm^{-1}, but, it is also very characteristic of tetrasilicic phases.

Micas with a very low tetrahedral charge, like bityite, $Ca(Al_2Li)(Si_2AlBe)O_{10}(OH)_2$ have a very different spectrum in that region. The salient feature is the presence of a very intense band at low wavenumber (close to 900 cm^{-1}) and of a weak band at a higher wavenumber : 1040 cm^{-1}. This situation is at the opposite of that previously encountered in tetrasilicic layer silicates and can be explained from similar structural considerations, based essentially on local charge balance considerations.

The same observations and conclusions are valid for amphiboles, with some noticeable exceptions. Most amphiboles with a free A-site are tetrasilicic; all of them exhibit their major intensity Si-O stretching band in the range 1040 - 1060 cm^{-1}: 1046 cm^{-1} in glaucophane, 1037 cm^{-1} in cummingtonite, 1040 cm^{-1} in anthophyllite, 1053 cm^{-1} in actinolite and 1058 cm^{-1} in tremolite, whereas amphiboles with an occupied A-site have their main intensity band at higher wavenumbers: 1072 cm^{-1} in Na-richterite and 1080 cm^{-1} in K-richterite. The characteristics of these alkaline-amphiboles are close to that of tetrasilicic micas, in this wavenumber range.But,the existence of two sets of Si-O stretching vibrations, one at high wavenumbers (above 1000 cm^{-1}) and one at lower values (below 1000 cm^{-1}) clearly reflects the existence of two kinds of tetrahedra: the small T(2) with high Si-O wavenumbers and the larger T(1) with lower wavenumbers. IR absorption gives similar informations; specially, the high-wavenumber band (≈ 1100 cm^{-1}) is sistematically observed .Numerous satellite Si-O stretching bands are visible in Raman and IR, around high- as well as low-wavenumber bands, in agreement with the known distortions of tetrahedra.

In K-richterite, the presence of tetrahedrally coordinated Ti^{4+} is detectable by the characteristic Ti-O stretching wavenumber at 897 cm^{-1} (Raman), calculable from the Si-O stretching frequency, and taking into account the variation of the reduced mass provoked by the Si-Ti substitution.

The domain of Si-O-Si and Si-O-Al vibrations.

In layer and chain silicates, these vibrations are active in IR (Au symmetry), with a very low intensity and in Raman (Ag symmetry), with a very high intensity; it is commonly the most intense band of Raman scattering spectra. The wavenumbers of these bands evolve in the same way with compositions, in IR and Raman, but only the Raman data offer a practical interest.

The study of selected peculiar compositions allows an unambiguous assignment of these bands. In the tetrasilicic magnesium mica $KMg_{2.5}Si_4O_{10}(OH)_2$, its wavenumber is 695 cm^{-1}; considering the tetrahedral composition of this mica, we can conclude that it is a pure Si-O-Si band. In the high-Al Na-mica preiswerkite $Na(Mg_2Al)(Si_2Al_2)O_{10}(OH)_2$, the major intensity band is observed at 651 cm^{-1}; here again, the tetrahedral composition allows the assignment: this band is due to the Si-O-Al vibration and indicates a strong Si,Al ordering, however, a minor-intensity band is also observed, at 676 cm^{-1} (Si-O-Si) and proves that this ordering is not complete. Micas with varied Al^{IV} contents fit in with these observations and exhibit a high-wavenumber Si-O-Si band and a low-wavenumber Si-O-Al band, e.g., 680 and 652 cm^{-1} in phlogopite. The

relative intensities of these bands are a function of the proportion of arrangements Si-O-Si and Si-O-Al. The A-site occupancy has a major effect on these wavenumbers; in talc $Mg_3Si_4O_{10}(OH)_2$, a tetrasilicic phase with a vacant A-site, this wavenumber (Si-O-Si) is only 676 cm^{-1}, that is, equal to the Si-O-Si wavenumber of preiswerkite. This observation is a further argument on behalf of the proposed assignment and emphasizes the fundamental role of the bulk number of charges adjacent to a bridging oxygen.

These conclusions apply surprisingly well to amphiboles: in the tetrasilicic alkaline amphibole K-richterite, this vibration is observed at 681 cm^{-1}, but it occurs at lower wavenumbers (similar to talc), in amphiboles with vacant A-site: 674 cm^{-1} in gedrite, 668 cm^{-1} in cummingtonite, 673 cm^{-1}, 673 cm^{-1} in anthophyllite, 671 cm^{-1} in glaucophane and 670 cm^{-1} in tremolite.

The low wavenumber range:below 600 cm^{-1}

Below 600 cm^{-1}, the structural informations that can be drawn from vibrational spectrometries are much more difficult to get,because a lot of phenomena overlap: low-energy angular vibrations of the pseudo-hexagonal ring of tetrahedra and stretching vibrations within octahedra. Owing to these intricacies, IR spectra usually exhibit broad, poorly resolved bands, whose interpretation is rarely unambiguous, whereas Raman spectra are frequently of low intensity in this range. It is generally possible to distinguish trioctahedral from dioctahedral phases in layer silicates; some characteristic spectra will be presented. It is also possible, in most cases, to identify the major octahedrally coordinated cations.

Far infrared measurements (150 cm^{-1} and below) are promising to qualify A-O bonds and resulting distortions of the A-site, but Raman measurements in th same wavenumber range cannot provide these informations since bands at wavenumbers close to 100 cm^{-1} are observed in talc (A-free phase) and in phlogopite (alkaline mica); the same observation is valid for amphiboles. These low-wavenumber bands are certainly due to translational movements of atomic groups, e.g., octahedra.

SOME CONTRIBUTIONS OF SPECTRAL STUDIES IN THE VISIBLE (AND NEAR-VISIBLE) LIGHT REGION TO MINERALOGY

David J. Vaughan, Department of Geology, The University, Manchester M13 9PL, England.

The absorption of energy in the visible (and nearby) regions of the electromagnetic spectrum is responsible for the colour of minerals and, in the special case of polarized light, for the (petrographic) phenomena of pleochroism and bireflectance. Quantification of these most accessible of spectra, combined with the development of theories for the origin of the absorption, offers explanations for optical properties and their variations, and a means of obtaining crystal chemical information. In this presentation, experimental approaches to the measurement of the absorption of visible/near-visible light energy, the origins of the absorption, and the applications of such measurements to mineralogical problems will be briefly reviewed.

The highest quality spectra are obtained from transmittance measurements on oriented single crystals in polarized light. Conventional spectrometers can be employed for measuring larger samples, but much of the available data have been obtained using microscope spectrophotometers (1, 2, 3), even though convergent microscope optics compromises the orientational purity of the incident light (4). Powdered samples of small grain size materials and opaque phases can be studied by diffuse reflectance spectroscopy (5, 6), although the resolution is much poorer. Single crystals of opaque minerals can be studied by specular reflectance measurements of polished surfaces using microscope photometers; generally, however, such spectra have been acquired for only the visible region (6, 7, 8).

The processes that contribute to the absorption of light in the visible and near-visible regions by minerals generally involve electronic transitions (although some contributions may arise in the near-infrared from overtones of vibrational transitions). The major contributions are from:

(i) Electronic transitions involving electrons in the *d* orbitals of transition metal ions. The degeneracy of the *d* orbitals is removed when these ions are placed in a crystalline environment. In the formalism of crystal field theory (1), the surrounding anions are treated as point charges and the effects of this field of charge on *d* orbital energies calculated. The gross assumptions involved in crystal field theory are counterbalanced by the ability to treat many electron systems and to assign spectral features due to *d*–*d* (crystal field) transitions.

(ii) Metal-metal (or intervalence) charge transfer transitions involving transfer of electrons between metal ions in different oxidation states (e.g. $Fe^{2+} \rightarrow Fe^{3+}$; $Fe^{2+} \rightarrow Ti^{4+}$; $Ti^{3+} \rightarrow Ti^{4+}$) and occupying adjacent sites in a crystal structure. Generally, pairs or clusters of the cations involved are in coordination polyhedra that share edges.

(iii) Ligand-metal charge transfer transitions involving electron transfer between anion and cation (e.g. $O^{2-} \rightarrow Fe^{3+}$). These are commonly centred at energies in the near-ultraviolet region of the spectrum.

(iv) Transitions involving energy bands, as in metals and semiconductors, where electrons can be excited from a valence band into large numbers of closely-spaced vacant energy levels in a conduction band, resulting in intense absorption.

In a few minerals, processes involving *f* orbitals (e.g. in uranium or rare earth-bearing phases) or various defects and imperfections (colour centres) are also important. The energies of charge transfer transitions can be described and predicted using molecular orbital theory, although certain limitations are imposed by what are generally "one-electron" models. The latter can also provide working models for certain of the opaque phases using a molecular orbital/band theory approach (6, 9).

The intensity of absorption is generally governed by quantum mechanically-derived selection rules that, for example, forbid electronic transitions between two *d* orbitals or two *p* orbitals, or that involve changes in the number of unpaired electrons on the cation. In practice, the rules are relaxed through mixing of orbitals and through various coupling and vibrational effects, so that transitions do occur but with greatly reduced probabilities and hence intensities. Site symmetries, particularly in the generally "distorted" cation sites found in many minerals, exercise an important control in this regard (1, 2, 5, 6).

Applications to mineralogical problems have included the use of detailed measurements of the polarized absorption spectra of translucent oriented single crystals to determine oxidation states, site occupancies and, in certain cases, concentrations of cations. An extensive list of published single crystal absorption spectra of minerals has recently been provided by Rossman (2). Previous authors have discussed the wider applications of such measurements to an understanding of mineral optics and crystal chemistry (1, 5, 6). Both single crystal absorption and diffuse reflectance spectra have been studied in order to interpret remote-sensed reflectance spectra, particularly of the terrestrial planets (5, 10); diffuse reflectance spectra have also been important in the characterization of fine-grained minerals such as clays and hydrated iron oxides (10, 11). The opaque oxide, sulfide and related minerals have been studied using diffuse reflectance spectroscopy, with the simpler phases being subject to more detailed specular reflectance measurements of single

crystals (6, 7 8) to gain insight into their electronic structures. Surface alteration effects in sulfides have also been studied by specular reflectance measurements (12). A very important area of development in recent years, dealt with in detail in another presentation, has been the study of absorption spectra at high pressures and temperatures.

Future developments in the application of spectral studies in the visible and near-visible light regions to minerals will likely involve single crystal absorption studies over a much wider range of pressures and temperatures, to monitor changes in crystal and electronic structure; further measurements of specular reflectance spectra of opaque minerals, also to relate to electronic structure models; and further diffuse reflectance studies of fine grained minerals and mixtures because of their importance in a variety of areas of applied earth science, particularly in remote sensing of planetary surfaces. A major challenge for the future, however, is the development of quantum mechanical theories to describe and predict the electronic transitions in minerals responsible for the absorption of energy in and near the visible light region. The continuing development of new algorithms and of more powerful computers should enable models of a much greater validity than, for example, crystal field theory, to be constructed (13).

References

(1) Burns, R.G. (1970). Mineralogical Applications of Crystal Field Theory. Cambridge Univ. Press.

(2) Rossman, G.R. (1988). Optical Spectroscopy. In Spectroscopic Methods in Mineralogy and Geology. Revs. in Mineralogy Vol. 18 (F.C. Hawthorne, ed). Min. Soc. Amer.

(3) Langer, K. & Abu-Eid, R. (1977). Measurement of the polarized absorption spectra of synthetic transition metal-bearing silicate microcrystals in the spectral range 44,000-4000 cm^{-1}. Phys. Chem. Mineral. *1*, 273-299.

(4) Goldman, D.S. & Rossman, G.R. (1979). Determination of quantitative cation distribution in orthopyroxenes from electronic absorption spectra. Phys. Chem. Minerals. *4*, 43-55.

(5) Karr, C. (1975). Infrared and Raman Spectroscopy of Lunar and Terrestrial Minerals. Academic Press, New York.

(6) Berry, F.J. & Vaughan, D.J. (1985). Chemical Bonding and Spectroscopy in Mineral Chemistry. Chapman and Hall, London.

(7) Vaughan, D.J. & Craig, J.R. (1978). Mineral Chemistry of Metal Sulfides, Cambridge Univ. Press.

(8) Criddle, A.J. & Stanley, C.J. (1986). The Quantitative Data File for Ore Minerals (Second Issue) British Museum (Nat. Hist.).

(9) Sherman, D.M. & Waite, T.D., (1987). Molecular orbital (SCF-X_α-SW) theory of metal-metal charge transfer processes in minerals. Parts I and II. Phys. Chem. Min. *14*, 355-363, 364-367.

(10) Burns, R.G. (1988). Spectral Mineralogy of Terrestrial planets: sampling their surfaces remotely (19th Hallimond Lecture). Mineral Mag. (in press).

(11) Schoonheydt, R.A. (1982). Ultraviolet and visible light spectroscopy (in clay studies). Dev. Sedimentol. *34*, 163-189.

(12) Vaughan, D.J., Tossell, J.A. & Stanley, C.J. (1987). The surface properties of bornite. Mineral. Mag. *51*, 285.

(13) Tossell, J.A. & Vaughan, D.J. (1988). Theoretical Geochemistry: Applications of Quantum Mechanics in the Earth, Mineral and Related Materials Sciences. Oxford Univ. Press. (in press).

DISTRIBUTION OF IONS IN PHYLLOSILICATES BY NMR SPECTROSCOPY.

J. SANZ.

Instituto de Ciencia de Materiales. CSIC. c/ Serrano 115-bis. Madrid 28006, Spain.

Nuclear magnetic resonance (NMR) is based on the absorption of electromagnetic radiation by an atomic nucleus in a magnetic field. The interaction of the magnetic moment of atoms with the applied magnetic field produces the splitting of energy levels of nuclei and the irradiation of sample with an adequate radio-frequency the resonant energy absorption. Moreover, the interaction of magnetic moment of nuclei with the local field created by the atomic environment produces characteristic modifications on the spectra which permit the identification of the sites occupied by atoms in the structure of the mineral. In general, from the analysis of the position of different lines it is possible to recognize the magnetic interaction of the nucleus with the environment and from that to deduce structural aspects related to chemical bond[1], coordination number[2], distortions of polyhedron[3], point symmetry[4], number of unequivalent sites[5]...

From the analysis of relative intensities of the identified components in the spectra it is possible to get information about sites occupation[6] and to analyze the relative distribution of ions in the mineral[7,8]. The application of the NMR spectroscopy does not require the existence of a regular periodic pattern and permit to study short range ordered distributions in crystalline samples that are difficult to be undertaken with diffraction methods, as the unit cell represent the average of all structural environments. On the other hand, the possibility of study different nuclei makes of the NMR a useful technique in the structural characterization of multicomponent systems where the determination of the site occupancies present serious difficulties by conventional diffraction methods[9]. However, spectroscopic methods and in particular NMR have its own area of application and should be viewed as complementary rather than mutually exclusive techniques.

In this contribution it will be analyzed the use of multinuclear NMR in the characterization of minerals. First, we shall present the advantages of the application of the new methods of high resolution (MAS technique, Cross-polarization, Decoupling...) in the study of structural environments of atoms. In the second part, we shall analyze the possibilities of conventional methods in the study of monocrystalline samples. We have chosen the phyllosilicates to illustrate the application of the NMR technique; in particular it will be discussed the distribution of isomorphous substitutions in the tetrahedral and octahedral sheet of these minerals and will be shown that, contrarily to what it is expected for such system a random distribution does not apply. The analysis of signals of different nuclei will permit the study of cation-cation, cation-anion and anion-anion distributions in theseminerals.

In the first part of this lecture, we present the results of high resolution ^{29}Si and ^{27}Al NMR study of well characterized phyllosilicates[10]. The spectra of powdered samples were recorded at 79.5 and 104.3 MHz respectively by spinning the sample at the magic angle 54°44' in a spectrometer Bruker MSL-400. The spinning frequency was in the range of 4000-5000 cps. Appropriate selection of samples has allowed to analyze the influence of different structural factors on the chemical shift of these nuclei. In samples with very low tetrahedral Al content the components detected in the ^{29}Si spectrum correspond to different crystallographic sites[11,12] The position of the line can be correlated with the angle TOT formed between contiguous tetrahedra. In this study, the use of cross-polarization technique permits the identification of silicon atoms in the structure that bear or are located near of OH groups. A particular application of the ^{29}Si NMR spectroscopy is the study of compounds where silicon tetrahedra have different degree of conectedness in the tetrahedral network.

In Phyllosilicates the substitution of Si for Al in neighbouring conected tetrahedra shifts the line of Si and permits the differentiation of Si atoms surrounded by 3Si, 2Si1Al, 1Si2Al and

3Al. The analysis of the relative intensities of the NMR components of ^{29}Si spectra, in samples with a wide range of compositions, provided useful information about Si,Al distribution in the tetrahedral sheet[13]. Several schemes of cation distribution have been considered and the comparison between experimental and model generated Si NMR intensities has permitted to prove that the Al distribution is more dispersed than required by the Loewenstein's rule (Al-O-Al avoidance) but clearly lower that that corresponding to the criterion of maximum dispersion of charges[14]. The most probable Si,Al distribution is one in which the number of Al per hexagonal ring is close to that given by the chemical composition. The proposed model of distribution has been confirmed by electrostatic energy calculations for samples with mica composition (Si_3Al)[15]. The electrostatic interaction between adjacent layers, conditions the Si,Al distribution in each layer and precludes the naximum dispersion of charges in these phyllosilicates.

The ^{27}Al MAS-NMR spectra of phyllosilicates consist of one or two components at ~ 0 ppm and ~ 70 ppm respectively that according to previous works[16] correspond to Al in octahedral and tetrahedral coordinations. In all the studied silicates tetrahedral Al is surrounded by 3Si and variations in the position of the line must be associated to the modifications in the TOT angle[17]. In the case of dehydroxylated phyllosilicates (caolin and pirophyllite) pentacoordinated aluminium is detected in intermediate positions ~ 30-40 ppm[18]. A quantitative determination of different types of Al is difficult as a consequence of the second order quadrupolar effects and more work must be done in this field.

In the next part of this lecture we shall present the study of octahedral sheet of the phlogopite-biotite serie. In these minerals Fe^{2+} substitutes for Mg^{2+} and OH^- can be replaced by F^-. The samples studied were chosen in order to have a practically continuous range in iron (0-20%) and fluorine (0-5%) contents. Fluorine and proton are nuclei which can be readily detected by NMR and its study has permitted to analyze the relative distribution of Fe^{2+}, F^- and OH^-. Experiments at high frequencies (60 and 54.6 MHz) allow to study the paramagnetic influence of varying Fe^{2+} contents in ^1H and ^{19}F signals, while experiments at low frequency (14 MHz) give information about diamagnetic interactions. The study was principally carried out at various angles around a and b axes in monocrystalline samples.

The analysis of ^{19}F spectra for different orientations of the sample has permitted to detect two doublets which correspond to pairs F-H and F-F in the same octahedron M_2[19]. The comparison of NMR intensities of the two doublets with the statistical values obtained from the mineralogical formulae shows that the number of F-F pairs increase much faster with F^- content than expected, which is interpreted as evidence for the existence of fluorine rich domains.

The effect of the interaction between nuclei (H,F) and the unpaired electrons of Fe^{2+} ions is to create at the nuclear site a supplementary field which shifts the measured frequency of the line. In the case of ^1H, the analysis of the position of different components with respect to the sample orientation has permitted the indentification of OH groups coordinated to the Fe^{2+} ions[20]. In the case of ^{19}F signal no lines corresponding to first neighbours have been detected, indicating that F^- ions are not directly coordinated to ferrous ions. When the external magnetic field is disposed perpendicular to the sheet plane, four lines are observed in the ^1H spectra, corresponding to OH coordinated to 3Mg, 2Mg1Fe, 1Mg2Fe and 3Fe. From the comparison of the intensities of these components with the values calculated on the basis of the random distribution of octahedral cations, it is concluded that the preferential association of F^- with Mg^{2+} ions in fluoro-magnesium domains is responsable of the accumulation of Fe^{2+} ions around OH^- groups in hydroxylated regions[7].

Finally, it is worthy to note that the application of multinuclear NMR spectroscopy has permitted to detect two different types of short range ordered distribution of cations in phyllosilicates, which are difficult to be analyzed by other methods. The presence of two anions (OH,F) in the octahedral sheet favours the segregation of microdomains in which the Fe-F avoidance is strictly verified. On the other hand, the homogeneous dispersion of Al makes unlikely the existence of tetrahedral cation segregation and favours the detected avoidance of Al in neighbouring tetrahedra known as the Loewenstein's rule.

REFERENCES

1. Smith K.A., Kirkpatrick, R.J., Oldfield E., Henderson D.M. (1983), Am. Mineral, 68, 1206
2. Engelhardt G., Michel D., in "High resolution solid state NMR of silicates and zeolites", John Wiley & Sons, NY, 1987 485 p.
3. Ghose S., Tsang T., (1973), Amer. Mineral. 58, 748
4. Tsang T., Ghose S. (1977), J. Chem Phys. 56, 3329
5. Fyfe C.A., O'Brien J.M., Srobl H., (1985) Nature, 326, 281
6. Klinowski J., Anderson M.W, (1986) J. Chem. Soc. Faraday Trans I, 82, 569.
7. Sanz J., Stone W.E. (1983), J. Phys. C.: Solid State Phys. 16 1271
8. Herrero C.P., Sanz J., Serratosa J.M. (1985) Solid State Comm. 53, 151
9. Hawthorne F.C. (1983). Amer. Mineral. 68, 287
10. Sanz J., Serratosa J.M. (1984), J. Amer. Chem.Soc., 106, 4790
11. Barron P.F., Frost R.L. (1985), Am. Mineral. 70, 758
12. Rojo J.M., Sanz J., Ruiz-Hitzky E., Serratosa J.M. (1986) Z. Anorg. allg. Chem. 540/541, 227
13. Herrero C.P., Gregorkiewitz M., Sanz J., Serratosa J.M., Phys. Chem. Minerals 15, 84
14. Herrero C.P., Sanz J., Serratosa J.M., J. Phys. Chem., submitted
15. Herrero C.P., Sanz J., Serratosa J.M. (1986), J. Phys. C: Solid State Phys. 19, 4169
16. Müller D., Gessner W., Behrens H.J., Scheler G. (1981), Chem. Phys. Lett 79, 59
17. Lippmaa E., Samoson A. Mägi M. (1986) J. Amer. Chem. Soc. 108, 1730
18. Madani A., Sanz J., Serratosa J.M., Moya J.S., Aza S. (1988) J. Amer. Ceram. Soc., in press.
19. Sanz J., Stone .W.E. (1979), Amer. Mineral 64, 119
20. Sanz J., Stone W.E. (1977), J. Chem. Phys. 67, 3739

Nuclear magnetic resonance spectroscopy and Al,Si ordering in minerals.

Andrew Putnis, Department of Earth Sciences, University of Cambridge, Cambridge, CB2 3EQ, England, UK.

NMR spectroscopy is an element-specific technique which probes the local (nearest and next-nearest neighbour) structural and chemical environment of a particular nucleus. Recent theoretical and experimental developments in high resolution NMR of solids, and the commercial availability of high-field Fourier Transform NMR spectrometers has led to a dramatic increase in the importance of this technique in modern mineral studies.

1. Background theory and terminology.

(i) Magnetic resonance.

The general field of magnetic resonance involves the interaction of magnetic moments with an applied magnetic field. Most nuclei have magnetic moments due to spin, denoted I. When a nuclear spin with a magnitude I is placed in a strong magnetic field, 2I + 1 energy levels exist, from -I to +I. When I = 1/2 as in ^{29}Si, the nucleus has two energy levels -1/2 and +1/2 and behaves as a magnetic dipole; when I > 1 the nucleus has more than two energy levels and behaves as a magnetic multipole.

The differences in nuclear energy levels are in the radio frequency range, and transitions between spin states may be induced by applying a radio frequency field to the sample in a large static magnetic field.

(ii) Chemical shift.

All nuclei of the same isotope in the same static magnetic field should have the same resonance frequency. However the exact resonance

frequency depends on the local electronic environment of the particular nucleus, because electrons in the vicinity of the nucleus shield it to varying degrees from the applied magnetic field. Thus the local chemical and structural environment can be probed by a nuclear method.

The resonance frequencies are reported as *chemical shifts,* which are differences in parts per million (ppm) relative to a suitable standard (for ^{29}Si the standard used is tetramethyl silane, $(CH_3)_4Si$ (TMS)). Each peak in the ^{29}Si NMR spectrum represents Si in a specific chemical environment, and the intensity is proportional to the number of atoms in that environment.

(iii) Magic angle spinning NMR.

NMR spectra in solids are broadened by dipolar and quadrupolar interactions which may be so strong as to obscure all structural information, and techniques have been sought to obtain high resolution spectra by removing these broadening effects. The most popular approach is magic angle sample spinning (MAS NMR) which involves physically spinning the sample at kilohertz frequencies about an axis oriented at 54.7° (the magic angle) to the applied static field. Since dipole - dipole interactions, which are a major cause of line broadening, are described by equations which contain $(3\cos^2\theta - 1)$ terms where θ is the angle between the laboratory field and the internuclear vector, they may be reduced to zero when $\theta = 54.7°$. Resonance peaks almost as narrow as in liquids may be obtained.

First order quadrupole interactions are also averaged, although if quadrupole coupling constants are large, line broadening is only partially averaged by sample spinning. The interpretation of spectra is considerably more straighforward for dipolar nuclei such as ^{29}Si. Most work on MAS NMR in minerals has concentrated on ^{29}Si which can also be observed at natural abundance (4.7%).

2. ^{29}Si MAS NMR

The first investigation of ^{29}Si MAS NMR spectroscopy of minerals was by Lippmaa and co-workers in 1980 who investigated a range of silicate structures with different polymerization states. A correlation was found between more negative chemical shifts and increasing degree of polymerization. In framework aluminosilicates ^{29}Si chemical shifts have been found to fall into five ranges depending on whether a given SiO_4 tetrahedron is linked to four, three, two, one or no AlO_4 tetrahedra. There is a constant and additive effect on the shift of about 5ppm for each aluminium atom added to the local environment.

Peak areas under such spectra are directly proportional to the total number of Si atoms in each distinguishable site. This is the key for determining Al,Si ordering schemes from ^{29}Si spectra.

For framework silicates Si/Al ratios may also be simply derived from the spectra, and in disordered Al-rich aluminsilicates the number of Al-O-Al linkages can also be derived forming a valuable basis for describing the degree of Al,Si order.

Empirical correlations of ^{29}Si chemical shifts.

It is not yet possible to calculate the magnitude of the chemical shift for any particular local structural environment, and various empirical relationships have been drawn from the databases of NMR spectra of materials with known composition and structure. The variations in chemical shifts for a particular nuclide appear to be due primarily to bond angle, bond length differences in the nearest and next-nearest neighbour co-ordination.

^{29}Si site assignments.

To illustrate the general approach currently used to assign sites in ^{29}Si MAS NMR spectra a number of examples will be discussed, ranging from

cases where unambiguous assignments can be made to minerals whose low symmetry and structural complexity make assignments difficult. Well ordered structures have the simplest spectra. Increasing the degree of Al,Si disorder increases the number of chemically non-equivalent sites producing distinguishable NMR chemical shifts.

3. Si assignments in ordered cordierite $MgAl_4Si_5O_{18}$.

Cordierite is a particularly good example to illustrate the application of ^{29}Si NMR spectra to Al,Si ordering, primarily because the somewhat unusual structure contains two very distinct Si environments in the fully ordered form resulting in a large difference in the chemical shift for the two Si peaks. When Al,Si disorder is introduced the resultant splitting of the peaks still allows eight different Si environments to be resolved in the spectrum.

When cordierite glass is crystallized at temperatures above 1100°C, the first phase to crystallize is hexagonal cordierite which can have no long-range Al,Si order. Subsequent annealing increases the degree of order until ultimately the stable structural state is fully ordered orthorhombic cordierite. The sequence of ^{29}Si NMR spectra for this process will be discussed.

Measurement of the peak intensities allows the quantitative determination of the population and depopulation of all the individual sites during the Al,Si ordering process in terms of individual local Si environments, information not available by other techniques.

The NMR data can also be used to demonstrate the existence of Al-O-Al bonds in partly ordered cordierites. The number of Al-O-Al bonds is progressively eliminated as the degree of order increases, and can be used as an order parameter Q_{od}, to define the temperature - time evolution of the cordierite structure, as well as to constrain models of short-range Al,Si order.

Correlation of NMR with X-ray synchrotron data in cordierite.

One of the problems in studying an Al,Si ordering process of this type, in which ordering results in a symmetry change, is to define the point at which the structure transforms on a macroscopic scale to the low symmetry form and to relate this to the degree of Al,Si order. X-ray synchrotron radiation was used to monitor the lattice distortion associated with the structural phase transition. This is defined by an order parameter Q which is determined by the spontaneous strain.

The relationship between Q and Q_{od} for all the structural states may be seen on an order parameter vector diagram. The main conclusion is that cordierite achieves a high degree of local Al,Si order while still macroscopically hexagonal. The intervention of a strain-modulated hexagonal phase, observed by transmission electron microscopy accomodates this local order within an overall hexagonal structure.

Correlation of NMR with IR spectroscopy in cordierite.

The time evolution of the Al,Si ordering and the structural phase transitions (hexagonal to modulated to orthorhombic) can be studied by monitoring the line profiles of various absorption peaks. Their integrated intensities, frequencies and half-width are correlated with the order parameters Q, Q_{od} and their short-range analogues. The phonon mode near 580 cm^{-1} correlates with the behaviour of Q and splits at the structural phase transition, whereas the mode around 770 cm^{-1} changes frequency linearly with log time, thus following the behaviour of Q_{od}, the degree of Al,Si order. By calibrating this frequency shift against the NMR data the number of Al-O-Al bonds as well as the degree of local structural distortion can be obtained from the IR spectrum.

Phase transformations in minerals studied by ^{57}Fe Mössbauer spectroscopy

Friedrich Seifert

Bayerisches Geoinstitut, Postfach 101251, D-8580 Bayreuth, FRG

ABSTRACT

Mössbauer spectroscopy can be a useful tool to characterize differences in geometry and bonding of an Fe-bearing site between two polymorphs and to determine changes in long-range and short-range order parameters as a function of temperature. In-situ measurements at pressure and/or temperature allow the determination of fast transitions such as rotative or distortive transformations, electronic transitions and magnetic ordering phenomena. Examples for individual successful applications of Mössbauer spectroscopy to mineral phase transitions are discussed.

1. INTRODUCTION

Phase transformations in minerals are critical to our understanding of the state and processes within the earth. They define the fields of stability of minerals as a function of pressure, temperature and other intensive variables. Given the appropriate chemical constraints, this equilibrium aspect teaches us which structures and assemblages we may expect as a function of depth, and, as a consequence, which physical properties (such as density, elasticity, conductivity) should prevail there. Furthermore, the kinetics of such phase transitions may elucidate the dynamics of processes in the earth (e.g. superplasticity, earthquake generation by sudden volume changes).

An understanding of phase transformations can only be achieved on a structural, i.e. atomistic, basis. Mössbauer spectroscopy is one useful tool for such a characterization, and in the following its applicability - or lack thereof - will be discussed.

It is not the purpose of this article to present a comprehensive review of the basics of Mössbauer spectroscopy nor of its application to mineralogy in general, because a number of summaries on this subject have been published recently (e.g. Maddock 1985, Hawthorne 1988). Rather, we will examine the Mössbauer parameters first with respect to their potential information on phase transitions, and then describe specific applications. Although many of the heavier nuclei exhibit the Mössbauer effect, we will deal with ^{57}Fe only because it is the geochemically most relevant nucleus.

2. MÖSSBAUER PARAMETERS

Mössbauer spectroscopy is element-specific, similar to nuclear magnetic resonance or X-ray absorption spectroscopy. It measures the interaction between the active nucleus and the extra-nuclear electric and magnetic fields. These features imply that, in a structural phase transition, only the changes in the immediate surroundings of the Mössbauer-active nucleus (such as changes in the coordination geometry, bonding etc.) will become visible in the spectra. In view of the localized nature of the information, the use of supplementary techniques is in general mandatory for characterizing a phase transition.

2.1. Debye-Waller factor

The Debye-Waller factor gives the fraction of gamma ray absorptions that occur without recoil relative to the total absorptions. Together with the concentration of the nucleus it controls the intensity of a Mössbauer line. It can be expressed as

$$f = \exp - k^2 \langle x^2 \rangle$$

where k is the magnitude of the wave vector of the gamma ray ($k = 2\pi/\lambda$, λ = wavelength) and $\langle x^2 \rangle$ is the mean square vibrational amplitude of the absorbing nucleus. f is thus also a function of temperature, pressure, and bonding, and may therefore be different for a given nucleus in different sites of a crystal structure. This aspect is important when a phase transition involves substitutional order-disorder phenomena (see below) and precise distribution coefficients between sites have to be determined. We note in addition that phase transitions exhibiting an increase in coordination number will increase $\langle x^2 \rangle$ (Navrotsky 1980) and thus result in a decrease in f. - Whereas ratios of f values (such as necessary in order-disorder studies) can be measured rather precisely from samples of known iron contents per site - such as pure iron end members - absolute determinations of f values are difficult and in general not precise enough to yield information on changes of $\langle x^2 \rangle$ in a phase transformation.

The temperature dependence of f also implies that in-situ observations of high temperature phase transitions (say, above 1000 K) are difficult to achieve by Mössbauer spectroscopy since the signal to noise ratio in the spectra deteriorates rapidly as temperature goes up and f goes down.

2.2. Line shape and line width

The energy distribution of a Mössbauer line around a central energy E value is, in theory, a Lorentzian distribution that can be described by E, the half width Γ (=0.194 mms^{-1} for ^{57}Fe) and the intensity (or, more precisely, fractional dip). This is

strictly valid only if an absorption is caused by a nucleus in a single, well-constrained crystallographic site and if the absorber is infinitesimally thin.

A number of effects tend to increase this halfwidth, even if there is no instrumental broadening. Most important are saturation effects (due to the non-zero concentration of the nucleus in a real sample), relaxation processes, fluctuating environments due to phase transitions, associations of defects etc. Line broadening also becomes apparent whenever a site is not strictly defined (in terms of geometry, bonding etc.) but actually a distribution of sites is present such as in glasses or by a multitude of next-nearest neighbors interactions. In such cases many authors still choose to describe a Mössbauer line by a (broadened) Lorentzian line, although a different treatment of the data such as a distribution of individual Lorentzian lines might be more appropriate (e.g. Wivel and Mörup 1980).

In practice, line widths up to about 0.30 mms^{-1} are still considered satisfactory. For broader lines it is often difficult to decide from the individual spectrum alone whether these should be fitted to two or more narrower lines or a single broadened line. This will become particularly important in the case of distortive and rotative phase transitions (see below) in which two distict sites merge into a single site as the transformation temperature is attained and the resolution of Mössbauer lines approaches zero.

In general, Mössbauer spectroscopy and its application to phase transitions with only minor structural changes suffers from low resolution, i.e. the separation of lines is often in the same order of magnitude as the line width. It has been shown by Dollase (1975) that reliable information on peak positions and peak areas can only be retrieved from a spectrum if line separation is at least 0.6 times the half width.

2.3. Isomer shift

The mean energy of the absorbed γ-radiation is affected by the interaction of the nuclear charge distribution with the electron density at the absorbing nucleus. Therefore, the maximum absorption in a sample A occurs generally at a different energy than emission of the source S:

$$\delta = C\partial R/R[|\psi_A(0)|^2-|\psi_S(0)|^2]$$

where δ = isomer shift, C = constant for a given nucleus, $\partial R/R$ is the change of nuclear radius between excited and ground state, and the term in brackets is the difference in electron density at the nucleus between absorber and source. With $\psi_S(0)$ generally constant, δ presents a direct though only relative measure of the electron density at the site of the nucleus. It is affected by the valence of the atom and its bonding (e.g. coordination number, electronegativity of the surrounding atoms, covalency effects, metal-anion distances). In the following, isomer shifts will always be reported relative to metallic iron.

For ^{57}Fe, $\partial R/R$ is negative, and δ increases with decreasing s-electron density at the nucleus. p and d electron indirectly affect $\psi(0)$ by shielding and the isomer shift is therefore an indicator of oxidation number and coordination.

For high-spin Fe^{2+} and Fe^{3+} the following approximate ranges have been reported for minerals (relative to Fe metal, at room temperature)

coordination	Fe^{2+}	Fe^{3+}
[4]-square planar	0.75 mms^{-1}	-
[4]-tetrahedral	0.60-1.10	0.10-0.35
[5]	0.84-1.11	-
[6]	1.05-1.25	0.36-0.55
[8]	1.20-1.40	-

Although there is some overlap between the ranges, coordination numbers generally can be assigned from isomer shift values. We note that Fe^{2+} exhibits a larger variation, and its isomer shifts are more sensitive to the environment of the nucleus than those of Fe^{3+}. The table also indicates that phase transformations involving a change in coordination number of Fe will be discernible by their Mössbauer spectra. At least for ferric iron phase transitions not affecting the coordination number of this atom will, on the other hand, only produce changes in the isomer shift that are at best on the order of the half width of the lines, that is, a quantification will be difficult on the basis of the isomer shift alone.

2.4. Quadrupole Splitting

Whenever a Mössbauer active nucleus is surrounded by a non-cubic field, the nuclear excited states split into sublevels, and the magnitude of this splitting Δ is proportional to the nuclear electric quadrupole moment eQ and the Z component of the electric field gradient (EFG) tensor. For ^{57}Fe

$$\Delta = -\tfrac{1}{2} V_{zz}\, e\, Q\, (1+\eta^2/3)^{1/2}$$

with $\eta = (V_{zz}-V_{yy})/V_{zz}$ (asymmetry parameter). Note that for a given nucleus this equation still contains two unknowns (V_{zz} and η). These depend on the contribution by the external ligands (lattice contribution) and a valence contribution that may - as in the case of Fe^{2+} - also contribute to a distortion of the inner electrons and thus to an EFG.

The dependence of the quadrupole splitting on distortion of a octahedral site from cubic symmetry has been modelled by Ingalls (1964, cf. Fig. 1).

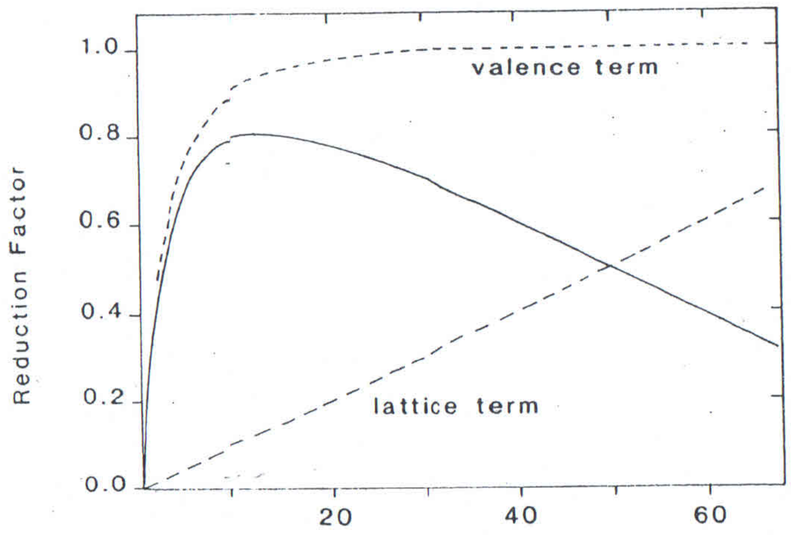

Fig. 1
Variation of quadrupole splitting of octahedral Fe^{2+} as a function of site distortion (after Ingalls 1964). The valence and lattice contributions are shown by the dashed lines, and the function resulting by subtracting the lattice from the valence contribution by the full line. The reduction factor represents the quadrupole splitting normalized to the maximum value of the valence contribution. Distortion of a site is defined by $\Delta/\lambda_0 a^2$, where Δ = splitting of the lowest crystal-field levels, λ_0 = spin-orbit coupling constant, α^2 = covalency factor. Note that the valence contribution and therefore the difference function are also temperature-dependent.

For Fe^{3+} the quadrupole splitting increases monotonically with increasing distortion, because for this spherically-symmetric ion only the lattice contribution is important. On the other hand, a maximum of the quadrupole splitting is attained for Fe^{2+}, due to the counteraction of a lattice and a valence contribution. This maximum of the quadrupole splitting is situated at rather low degrees of distortions. Most octahedral sites containing Fe^{2+} in silicates - possibly with the exception of the M1 site in pyroxenes (Dowty and Lindsley 1973) - seem to be so highly distorted that they plot to the right of the maximum in Fig. 1, and the larger quadrupole splittings are associated with the less distorted sites.

For any valence state and coordination the quadrupole splitting is therefore highly variable (ranging, for instance, from 0 to 3.20 mms^{-1} for ferrous iron in octahedral coordination) and presents a sensitive parameter that can be used in characterizing structural changes during phase transitions.

2.5 Nuclear Zeeman splitting

This splitting of levels originates from the interaction between the magnetic dipole moment of the nucleus and a magnetic field H at the nucleus. The splitting is proportional to the magnetic quantum number m_i, the nuclear Bohr magneton β_N, the nuclear Lande splitting factor g_N

$$E_m = -g_N \beta_N H m_i$$

In the ferromagnetic and antiferromagnetic states of minerals the direction of the field is fixed and magnetically split spectra occur below the Curie and Neel temperatures, respectively. In the paramagnetic state, on the other hand, the magnetic field fluctuates so rapidly within the lifetime of the excited state of the Fe nucleus that the average dield that the nucleus "sees" during the transition from the excited to the ground state is zero. The appearance of a split spectrum can therefore be used to characterize the onset of magnetic ordering (see below).

3. PHASE TRANSITIONS AND MÖSSBAUER SPECTROSCOPY

In the following, we will exclusively discuss phase transitions between individual structures of the same compositions, i.e. we will not deal with heterogeneous reactions involving more than two phases. Mössbauer spectroscopy has, for instance, extensively been applied to transformations between iron-hydroxides and anhydrous Fe_2O_3 (e.g. Chambaere and De Grave 1985) but treatment of such transformations is beyond the scope of this paper.

Phase transformations can be classified under several aspects - e.g. thermodynamic, structural, or kinetic. Because Mössbauer spectroscopy is a structural tool, we will use the classification proposed by Buerger (1961) and amplified by Liebau (1983). It is essentially a combination of the thermodynamic approach (Ehrenfest 1933) with the crystal-chemical aspect. In addition to that classification, phase transitions due to changes in the electronic and magnetic state will also be discussed. Only those transitions will be treated in some detail where Mössbauer spectroscopy can contribute to their characterization.

Application of Mössbauer spectroscopy to phase transitions is particularly advantageous in the following cases

a) in quenchable phase transformations to characterize the changes in coordination of Fe, and possibly its valence as well as its distribution over different sites of a structure

b) by in-situ measurements to determine the nonquenchable changes in the structure during the approach to a phase transition by changing pressure or temperature conditions

c) to characterize phase transitions that go undetected by standard techniques - such as electronic or magnetic transitions. These also require in-situ measurements

Whereas for the study of group a) transitions the conditions of the Mössbauer experiment can be adjusted so as to get the optimum resolution and signal to noise ratio, in-situ experiments at P and/or T are necessary for group b) and c) applications. The study of Mössbauer spectra under pressures up to several 100 kbars presents no major obstacles (e.g. Zou et al. 1980, Hayashi et al. 1987), if pressure gradients over the sample are avoided by the use of a hydrostatic pressure medium. On the other hand, temperatures above about 1000 K will drop the f-values (cf. above) and deteriorate the signal to noise ratio. High-temperature measurements are, therefore, in general only feasible in simple structures. Simultaneous applications of pressure and temperature are even more restricted.

Very often it would be desirable to follow the phase transformation as it occurs, in order to find short-lived intermediate structures or to determine the mechanism itself. Because accumulation of a Mössbauer spectrum takes on the order of 10 hours, this kind of spectroscopy is not well suited to watch the process as it occurs. Pressure scan or thermal scan methods - where the velocity of the Mössbauer drive velocity is kept constant and single-channel absorption is monitored in response to pressure or temperature - give only limited information.

4. SPECIFIC EXAMPLES

4.1. Structural Phase Transitions

4.1.1. Changes in the first coordination shell

Here we summarize phase transitions due to changes in the coordination number of at least one constituent cation. These may be either reconstructive, i.e. involve breaking of bonds, or dilatative, that is transformations can be achieved, at least on paper, by a continuous deformation of the reactant structure into the product structure.

If the iron-bearing positions themselves are affected by the changes in coordination number, we may expect major changes in the spectrum in such a transition, because of the strong dependence of hyperfine parameters on the first coordination shell.

a. reconstructive phase transitions

A number of mineralogically and petrologically most important phase transformations belong to this class, such as the high-pressure transitions of the $(Mg,Fe)SiO_3$ polymorphs from the orthopyroxene to the ilmenite, garnet, and perovskite structures, in which the coordination number of the ferrous iron increases from six in orthopyroxene and ilmenite to eight in garnet and eventually 12 in the perovskite structure. The Mössbauer data base for these transitions is, however, still extremely meager.

The aluminum silicates Al_2SiO_5 present an example of changing coordination numbers for some of the Al positions from 4 and 6 in sillimanite to 5 and 6 in andalusite, and exclusively 6 in kyanite. In all these modifications Fe^{3+} substitutes for only six-coordinated Al. Consequently, the changes in isomer shift are negligible, whereas the quadrupole splittings trace the changing distortion of the octahedral sites:

Polymorph	δ	Δ	Reference
sillimanite	0.37 mms-1	1.06-1.07	Halenius 1979
andalusite	0.35-0.36	1.73-1.81	Halenius 1978
kyanite	not determined	ca. 0.8	Parkin et al. 1977

A structural transition in melts (glasses) may be classified here as well, although in detail it is much more complex than most transitions in the solid state in well-defined structures. Mysen and Virgo (1985) used Mössbauer spectroscopy to determine the redox equilibria of iron and the structure of quenched melts in the system $Na_2Si_2O_5$-Fe_2O_3 up to 40 kbars. Two effects occur simultaneously with increase of pressure: the Fe^{3+} doublet(s) decrease in intensity relative to the Fe^{2+} doublet(s), and the isomer shifts of Fe^{3+} increase from ca. 0.30 mms^{-1} to ca. 0.6 mms^{-1}. This can be taken as evidence for a pressure-induced reduction of Fe^{3+} to Fe^{2+} and a concomitant coordination change of the remaining Fe^{3+} from tetrahedral to octahedral coordination. The oxygen produced by the reduction is thought to be dissolved in the melt in molecular form. - By this transition, the degree of polymerization of the melt is changed markedly, which, in turn, affects its physical properties such as viscosity. Clearly, in-situ measurements for such transitions would be preferable to studies of quenched melts.

b. dilatative phase transitions

Hazen and Finger (1983) described the changes in crystal structure of gillespite $BaFeSi_4O_{10}$ as a function of pressure. The coordination of Fe^{2+} in the low-pressure phase (gillespite I) is square-planar whereas in the high-pressure modification (gillespite II) it changes to a highly distorted tetrahedral coordination, with two other oxygens moving close enough that the coordination might also be considered as (4+2). These two longer bonds are particularly compressible, i.e. within the stability field of gillespite II octahedral coordination is approached with increasing pressure. High-pressure Mössbauer spectra of gillespite have been reported by Huggins et al. (1975, 1976). They noted little change in the hyperfine parameters near the I-II phase transition itself (δ = 0.79, Δ = 0.57 mms^{-1}, slightly depending on pressure), but a second doublet (with δ = 1.09 and Δ = 2.05 mms^{-1}) increasing in intensites at the expense of the gillespite I tetrahedral doublet within the stability field of the gillespite II phase. These parameters are close to those expected for octahedral ferrous iron (but not for Fe in the eight-coordinated barium site as suspected by Hazen and Finger 1983). A speculative interpretation of the Mössbauer spectra within the stability field of the gillespite II phase might thus be that a domain structure exists (undetected by X-rays) with some domains containing tetrahedral and others octahedral Fe, and that their proportions change with pressure.

4.1.2. Changes in the second coordination shell

As discussed in section 2. the influence of the second coordination shell on hyperfine parameters is, in general, only slight and we will not expect major changes in the Mössbauer spectra during phase transitions of this kind.

a. Reconstructive phase transitions

The olivine-spinel transformation in Fe_2SiO_4 may be taken as an example, because Fe remains in octahedral, and Si in tetrahedral coordination. As predicted, the change in hyperfine parameters (at room temperature, where M1 and M2 in olivine are not resolved) is only minor (Huggins et al. 1975):

	olivine	spinel
δ	1.15 mms^{-1}	1.16
Δ	2.78	2.61

b. displacive phase transformations

No clear-cut examples for this type of transitions are known from Mössbauer studies, and the two folling cases might illustrate some of the basic difficulties of applying Mössbauer spectroscopy to such transitions. Both titanite, $CaTiSiO_5$, and $BaTiO_3$ show displacive phase transitions (Taylor and Brown 1976, Müller 1981), in which the Ti atoms are displaced from the center of the octahedra in the low-temperature phase. Fe^{3+} impurities substituting for Ti in titanite (Vassilikou-Dova and Lehmann 1988) seem to be concentrated in the domain walls of the low-temperature $P2_1/a$ phase, since their EPR signals are broadened. In $BaTiO_3$, Fe^{3+} impurities do not participate in the collective off-center motion of Ti^{4+} ions during the phase transition (Siegel and Müller 1979). - At least for some phase transitions of this kind severe limitations therefore exist in using Mössbauer spectroscopy of Fe as a low-concentration probe into the structural rearrangement. In addition, these transformations are so rapid that in-situ measurements would be necessary.

4.1.3. Phase transitions involving order-disorder

a. Substitutive phase transitions

In these transformations changes in the degree of ordering of different atoms (or atoms and vacancies) over at least two crystallographically distinct sites takes place as a function of temperature. Because bonds have to be rearranged in this process, it is generally slow, and the samples are quenchable. Upon disordering with increasing temperature, the low-temperature phase may become completely disordered at a well-defined temperature (convergent disordering) with a change in symmetry and/or unit cell size. A mineralogical example is the transition from a $Fe_{50}Ni_{50}$ ordered phase (Petersen et al. 1977) that occurs in some particularly slowly-cooled and Ni-rich meteorites, into the disordered γ-phase near 320°C (Danon et al. 1979). However, in minerals another (nonconvergent) disordering scheme prevails: Due to the topology of the structure, the two sites over which the disordering takes place would remain crystallographically distinct even at complete disorder (e.g. the tetrahedral and octahedral sites in the spinel structure) and theory then predicts that complete disorder could only be achieved at infinitely high temperatures.

One classical application of Mössbauer spectroscopy is the study of changes in ordering of two atomic species over two or more crystallographically distinct sites as a function of temperature in the partially ordered phase. In simple binary systems such as $Mg_2Si_2O_6$-$Fe_2Si_2O_6$ or $Mg_7Si_8O_{22}(OH)_2$-$Fe_7Si_8O_{22}(OH)_2$ resolution of the spectra is often very good and highly quantitative site occupancies can be extracted. Heterovalent substitutions (such as 2Al for Mg,Si) tend to blurr the spectra, however, probably due to next-nearest neighbors interactions. By quenching experiments, the temperature-dependent equilibrium cation distribution of Mg and Fe^{2+} over individual sites has been determined for e.g. orthopyroxenes (Virgo and

Hafner 1969, Saxena and Ghose 1971) and amphiboles (Seifert 1978, Skogby 1987), as well as the kinetics of the ordering or disordering processes (Besancon 1981 for orthopyroxenes, Seifert and Virgo 1975 for anthophyllite, Skogby 1987 for tremolite). Temperature-dependent order-disorder of Fe^{3+},Al between different octahedral sites in epidote has been reported by Dollase (1973).

The main use of Mössbauer spectroscopy is to obtain the long-range order parameter (described by a e.g. Mg-Fe^{2+} distribution coefficient K) as a function of temperature, heating duration and composition. Attainment of equilibrium can be proven by bracketing the K value through ordering and disordering experiments. The equilibrium values of K (T) permit the calculation of the Gibbs' Free Energy of the exchange reaction, which may then be used to define enthalpy and entropy values. For instance, Seifert (1977) showed that, in orthoamphiboles, Δ G depends both on temperature and composition: In Al-poor anthophyllites the entropy contribution to Δ G is large, but decreases systematically as even small amounts of Al (up to 0.42 per 22 oxygen) are incorporated into the structure (Fig. 2).

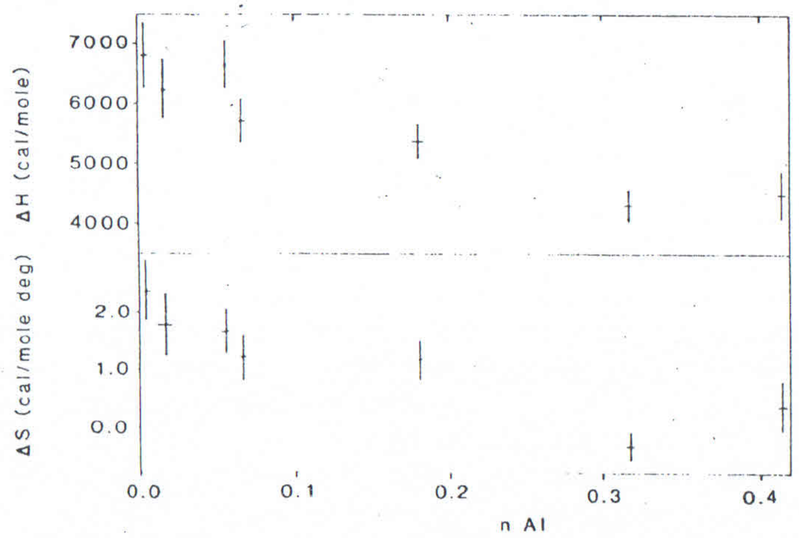

Fig. 2
Energetics of the long-range Fe-Mg ordering process in natural anthophyllites $(Mg,Fe)_7Si_8O_{22}(OH)_2$-$Na_{0.5}(Mg,Fe)_{5.5}Al_{1.5}$-$Si_6Al_2O_{22}(OH)_2$, as a function of Al content per 22 oxygens. Data taken from Seifert (1978)

This behaviour can be rationalized by considering the changes in bond lengths and site distortions as a function of Al content. By heating experiments at constant temperature but variable duration, the kinetic constants of the exchange process may be extracted from the changes in site-occupancies in addition. In principle, the combination of the equilibrium K(T) data and the rate constants allows the determination of the cooling rate of a mineral (Seifert and Virgo 1975, Besancon 1981, Saxena 1983, Skogby 1987). In practice, however, the method is still only semiquantitative for slowly-cooled rocks, because extrapolation over large temperature ranges and durations are required, and it has to be assumed that the mechanism remains constant.

All these studies pertain to long-range order parameters. Mössbauer spectroscopy has, however, also the potential of determining short-range order, i.e. the clustering of species and/or defects. These become apparent in the spectra through next-nearest -neighbors interactions. Their effects on the spectra are strong when a cubic site is slightly distorted by a noncubic environment, because then the quadrupole splitting is very sensitive to minor changes in distortion (cf. Fig. 1). Therefore, next-nearest-neighbors interactions are clear-cut in e.g. wüstite, where they originate through vacancies and Fe^{3+} that set up a non-zero EFG at the octahedral Fe^{2+} site. Similarly, the quadrupole splitting of Fe^{2+} in spinels (e.g. in the system $FeCr_2O_4$-$FeAl_2O_4$, Bancroft et al. 1983) senses the concentrations of Al and Cr as next-nearest neighbors.

In silicates, on the other hand, polyhedra are in general already highly distorted and therefore the quadrupole splitting changes hardly in response to changes in next-nearest neighbour configuration (cf. Fig. 1). There are indications but no definite proof yet that considerable short-range order exists for Fe^{2+} in the M2 site and Al in the M1 site in orthopyroxenes (Seifert 1983). Resolution is, however, marginal and other methods such as EXAFS might prove to be more useful for determining temperature-dependent short-range order in such minerals.

Finally, there are transitions where the short-range order is preserved but the long-range order of the anionic part of the structure changes, such as in the P2/n - C2/c transition in omphacites. In these cases the Mössbauer spectra show no discernible changes during the transition (Aldridge et al. 1978).

b. Distortive and rotative transitions

An order parameter is defined in these transitions by the atomic displacements Δx (distortive) or rotation angle $\Delta\varphi$ (rotative) of polyhedra relative to their position in a high-temperature phase. It is often difficult to distinguish this type of transition (with two energetically equivalent structural states $+\Delta x$, $-\Delta x$, and $+\Delta\varphi$ and $-\Delta\varphi$) from displacive transitions with changes in the second coordination shell (see above). For instance, the high-low quartz transition has been classified in either way.

Phase transitions of this type are kinetically fast because no bonds are broken. They have, therefore, to be investigated under in-situ conditions.

An example of a rotative transformation has recently been studied through Mössbauer spectroscopy by Seifert et al. (1987) in melilites. Fe-doped akermanite undergoes a reversible phase transition at 85 °C (Hemingway et al. 1986) that becomes apparent in the Mössbauer spectra by a single Fe doublet in the high-temperature phase but a splitting into two doublets in the low-temperature phase. High-resolution electron microscopy and electron diffraction reveals that the low-temperature phase is a incommensurately modulated structure. Approaching the phase transition from the low-temperature side, the modulation wavelength increases and its amplitude becomes weaker. The hyperfine parameters of the two kinds of Fe indicate the presence of a "compressed" and a "expanded" tetrahedral site which become more similar with increasing temperature and merge into one as the phase transitions occurs at the critical temperature Tc (Fig. 3).

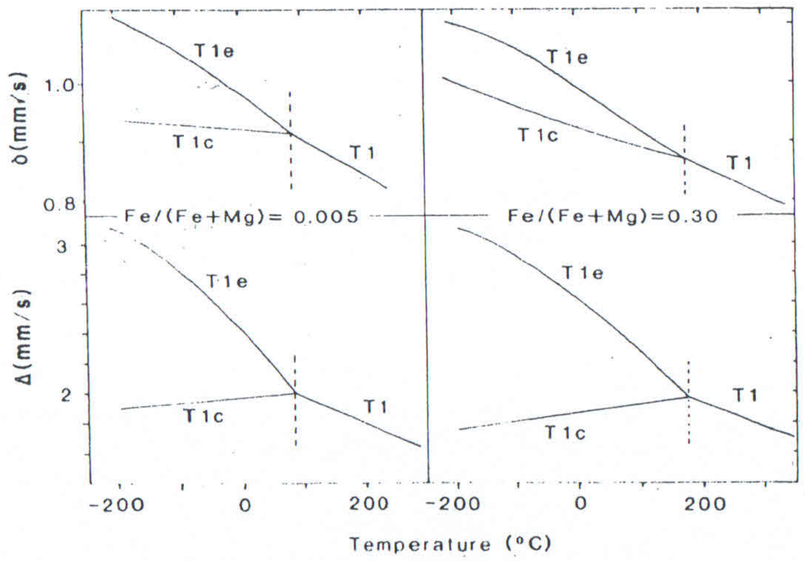

Fig. 3
Variation of hyperfine parameters in akermanites, $Ca_2(Mg,Fe)Si_2O_7$ as a function of temperature (data from Seifert et al. 1987). Note the splitting of the single T1 site (high temperatures) into two sites (T1e and T1c) at the phase transition near 85°C for Fe/(Fe+Mg) = 0.005 (left diagram) and near 170°C for Fe/(Fe+Mg) = 0.30 (right diagram).

Near the phase transition, it is hard to judge whether a two-doublet or a single-doublet fit should be employed because resolution is lost at Tc. Nevertheless, the exact Tc can be extracted from the Mössbauer spectra by examining the half-widths of the lines as a function of temperature.

For the phase transformation the following structural model has been developed (van Tendeloo, personal communication 1987): In the high temperature phase (S.G. P4 2_1m) the Si_2O_7 dimers are located on mirror planes and the two T1 positions (containing Mg,Fe) per unit cell are identical (Fig. 4).

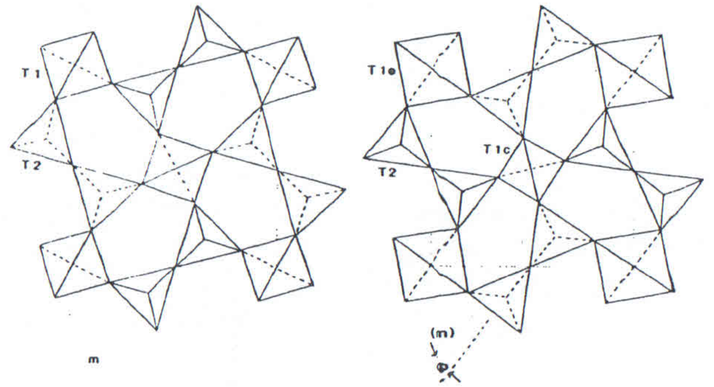

Fig. 4
Tetrahedral sheet in the high-temperature melilite phase (left, after Kimata and Ii 1981) and the low-temperature modulated phase (right) as proposed by van Tendeloo (personal communication 1987). The mirror planes (only one indicated by m) present in the high-temperature phase are destroyed in the low-temperature phase by a rotation φ of the Si_2O_7 groups, generating an "expanded" T1e and a "compressed" T1c site in which Mg and Fe are located.

At the phase transition, the mirror plane is destroyed and in the low-temperature phase the Si_2O_7 groups rotate away by an angle φ, and thereby create a "compressed" T1c and an "expanded" T1e site (Fig. 4). φ increases with decreasing

temperatures - explaining the increasing differences between T1c and T1e sites at low temperatures (cf. Fig. 4). Domains with rotations $+\varphi$ and $-\varphi$ define the observed incommensurate modulation. In detail, it is not yet clear whether the Si_2O_7 groups rotate as an entity (such as assumed in Fig. 4) or whether they also may become kinked at the bridging oxygen (F. Roethlisberger, unpublished results 1988).

4.2. Electronic transitions

Among these (cf. Drickamer and Frank 1973) the following are most important in minerals:

4.2.1. Intervalence charge-transfer transitions

If a structure contains transition elements that are capable of more than one oxidation state, then electrons may be transferred between states of one or several transition metal species by thermal activation. The Mössbauer effect "sees" an averaged electronic charge if the mean lifetime of the excited nuclear state (t = 141 ns) is long relative to the average time of residence of an electron at a given atom. In the case of Fe^{2+} - Fe^{3+} intervalence charge transfer the Mössbauer parameters are then intermediate between those of ferrous and ferric iron.

The "classical" example of such a transition is ilvaite, $Ca(Fe^{2+}Fe^{3+})Fe^{2+}Si_2O_8(OH)$ (cf. Ghose 1988). $Fe^{2+}O_6$ and $Fe^{3+}O_6$ form edge-sharing double chains of octahedra, and the exchange of electrons occurs between these sites. At room temperature and pressure only a weak Mössbauer doublet occurs that is indicative of "$Fe^{2.5+}$" but this doublet rapidly increases in intensity with both pressure and temperature (Litterst and Amthauer 1984). - It has been shown by Amthauer (1982) that such thermally activated exchange processes are confined to minerals having infinite edge-sharing chains of Fe octahedra (other examples are deerite, $Fe^{2+}{}_6Fe^{3+}{}_3O_3(Si_6O_{17})(OH)_5$, Amthauer et al. 1980 or bornite $Cu_{4.5}Fe_{1.2}S_{4.7}$, Jagadeesh et al. 1981, with Cu^{1+}-Cu^{2+}-Fe^{2+}-Fe^{3+} hopping), whereas in minerals with finite octahedral Fe clusters only optically-activated intervalence charge transfer may occur.

4.2.2. Spin changes in iron complexes

In oxide and silicate minerals Fe is exclusively in the high-spin state, whereas low-spin Fe^{2+} has been reported in some sulfide minerals (e.g. Jagadeesh et al. 1971). A phase transition involving a change from high spin to low spin as a consequence of increasing pressure has been described by Bargeron et al. (1971) for the synthetic equivalent of the mineral hauerite MnS_2 doped with 2% FeS_2 component (Fig. 5).

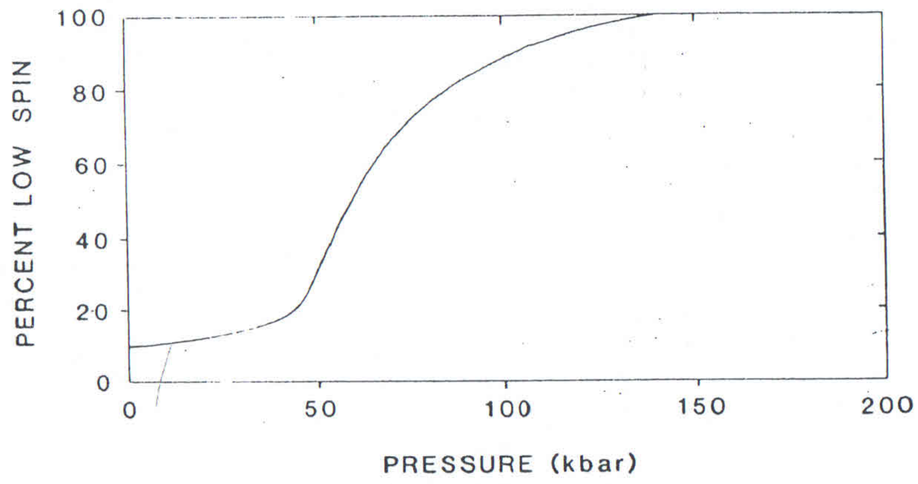

Fig. 5
Pressure-induced conversion of high-spin to low-spin Fe in hauerite, MnS_2. Data from Bargeron et al. 1971.

At 1 bar, Fe is in the high-spin state (probably because the Fe sites are dilated by the majority of the large Mn-filled sites in the structure) but upon increase of pressure the Fe undergoes a reversible transition to the low-spin state, being complete at 138 kbars. - Pressure-induced changes from the low-spin to the high-spin state have, so far, only be observed in organometallic compounds and cyanides (cf. Drickamer and Frank 1973).

4.3. Magnetic transitions

In the high-temperature paramagnetic state the field orientation changes rapidly compared to the mean lifetime of the excited state, but at low temperatures (about 20-50 K for most minerals) the relaxation becomes so slow that magnetic splitting is observed in the spectra. The cooperation interactions lead to parallel (ferromagnetic) or antiparallel (antiferromagnetic) couplings below the Curie and Néel temperatures, resepctively. An antiferromagnetically ordered structures, spin cauting with an angular displacement of the spins may define another (Morin) transition. Mössbauer spectra allow the determination of the magnitude of the internal field (cf. 2.5) and its variation with temperature. Types of magnetic ordering can be

distinguished by applying an external field (cf Hawthorne 1988), but supplementary techniques such as measurements of susceptibility and magnetization, or neutron diffraction are often employed for a full characterization. Antiferromagnetic ordering seems to be the most common in minerals. The pressure-dependence of the paramagnetic to antiferromagnetic transition in fayalite, Fe_2SiO_4, has been measured by in-situ Mössbauer spectroscopy by Hayashi et al. (1987) up to 160 kbars. The Néel temperature increases linearly with pressure according to an equation $T_N(K) = 65 + 0.22$ P (kbar).

In a combined Mössbauer and X-ray study Zou et al. (1980) determined the paramagnetic to antiferromagnetic transition in a wüstite of composition $Fe_{0.947}O$. At 50 kbars pressure (at room temperature) a magnetic sextett starts to develop, increasing in intensity relative to the paramagnetic line with increased pressure. In the same pressure range the cubic cell of the low-pressure phase distorts to a hexagonal phase. The phase transition may, therefore, be viewed as a combination of a magnetic with a structural dilatative transformation (cf. 4.1). This pressure-induced transition probably is identical to the one occurring at 1 bar, 198 K, but the magnitude of the change is considerably larger at pressure.

Grunerite, $Fe_7Si_8O_{22}(OH)_2$ shows onset of magnetic ordering at 47 K and further changes in the Mössbauer spectra near 7 K (Linares et al. 1983). Ghose et al. (1987) were able to assign this latter transition to a spin canting, on the basis of susceptibility and neutron diffraction measurements. Within the stability field of the antiferromagnetic phase spins within the octahedral bands are ferromagnetically coupled, but each band antiferromagnetically coupled to the neighboring bands.

5. CONCLUDING REMARKS

It has been shown by the examples above that Mössbauer spectroscopy may be a sensitive technique to determine and characterize various kinds of phase transformations, particularly when supplemented by other techniques. The main advantages are the sensitivity to changes in the electronic and magnetic properties and, in some cases, to the distortion of sites and long-range or short-range order parameters. With ^{57}Fe enriched synthetic samples, amounts corresponding to less than 0.1 mg Fe may be sufficient - quite in contrast to e.g. powder neutron diffraction methods. So far, in most in-situ studies only pressure or temperature have been varied. At least from the example of the paramagnetic-antiferromagnetic phase transition in wüstite (cf. Section 4.3) it is clear, however, that the magnitude of the change at a phase transition and possibly even its character and mechanism may change with pressure and temperature. For investigating phase transitions in PT-space, however, further methodological developements would be desirable, such as heated diamond-anvil cells or high-temperature (above 1000 K) systems. Eventually, the atomic motions during phase transformations might also become accessible through Mössbauer measurements, because of the diffusional broadening of lines. From this, either jump frequencies or jump distances may be extracted, and if the diffusion coefficient is known, the path of an atom may be traced during a transformation.

REFERENCES

ALDRIDGE L.P., G.M. BANCROFT, M.E. FLEET, C.T. HERZBERG (1978) Omphacite studies II. Mössbauer spectra of C 2/c and P 2/n omphacites. Am. Mineral. 63, 1107-1115

AMTHAUER G., K. LANGER, M. SCHLIESTEDT (1980) Thermally activated electron delocalization in deerite. Phys. Chem. Minerals 6, 19-30

AMTHAUER G. (1982) Gemischte Valenzzustände des Eisens in Mineralen. Fortschr. Mineral. 60, 119-152

BARGERON C.B., M. AVINOR, H.G. DRICKAMER (1971) The effect of pressure on the spin state of iron (II) in manganese (IV) sulfide. Inorg. Chem. 10, 1338-1339.

BANCROFT G.M., M.D. OSBORNE, M.E. FLEET (1983) Next-nearest neighbour effects in the Mössbauer spectra of Cr-spinels: an application of partial quadrupole splittings. Solid State Comm. 47, 623-625

BESANCON J.R. (1981) Rate of cation disordering in orthopyroxenes. Am. Mineral. 66, 965-973

BUERGER M.J. (1961) Polymorphism and phase transfromations. Fortschr. Miner. 39, 9-24, 1961

CHAMBAERE D.G., E. DE GRAVE (1985) The β FeOOH to α Fe_2O_3 phase transformation: structural and magnetic phenomena. Phys. Chem. Minerals 12, 176-184

DANON J., R. SCORZELLI, I. SOUZA AZEVEDO, W. CURVELLO, J.F. ALBERTSEN, J.M. KNUDSEN (1979) Iron-nickel 50-50 superstructure in the Santa Catharina meteorite. Nature 277, 283-284

DOWTY E., D. LINDSLEY (1973) Mössbauer spectra of synthetic hedenbergite-ferrosilite pyroxenes. Am. Mineral. 58, 850-868

DOLLASE W.A. (1973) Mössbauer spectra and iron distribution in the epidote group minerals. Z. Krist. 138, 41-63

DOLLASE W.A. (1975) Statistical limitations of Mössbauer spectral fitting. Amer. Mineral. 60, 257-264

DRICKAMER H.G., C.W. FRANK (1973) Electronic transitions and the high pressure chemistry and physics of solids. Chapman and Hall, London

EHRENFEST P. (1933) Phasenumwandlungen im üblichen und erweiterten Sinn, classifiziert nach den entsprechenden Singularitäten des thermodynamischen Potentials. Proc. Kon. Amsterdam Acad. 36, Suppl. 75b, 153-157

GHOSE S. (1988) Electron ordering and associated crystallographic and magnetic phase transitions in ilvaite, a mixed-valence iron silicate. In: S. Ghose, J.M.D. Coey, E. Salje eds. Structural and magnetic phase transitions in minerals. Springer Verlag, Heidelberg

GHOSE S., D.E. COX, N. VAN DANG (1987) Magnetic order in grunerite, $Fe_7Si_8O_{22}(OH)_2$ - a quasi-one dimensional antiferromagnet with a spin canting transition. Phys. Chem. Minerals. 14, 36-44

HALENIUS U. (1978) A spectroscopic investigation of manganian andalusite. Canad. Mineral. 16, 567-575

HALENIUS U. (1979) State and location of iron in sillimanite. N. Jb. Mineral Monatshefte 1979, 164-174

HAWTHORNE F.C. (1988) Mössbauer Spectroscopy in: F.C. Hawthorne ed. Spectroscopic Methods in Mineralogy and Geology. Reviews in Mineralogy 18, 255-340, Mineralogical Society of America, Washington D.C.

HAYASHI M., I. TAMURA, O. SHIMOMURA, H. SAWAMOTO, H. KAWAMURA (1987) Antiferromagnetic transition of fayalite under high pressure studied by Mössbauer spectroscopy. Phys. Chem. Minerals 14, 341-344.

HAZEN R.M., L.W. FINGER (1983) High-pressure and high-temperature crystallographic study of the gillespite I-II phase transition. Am. Mineral. 68, 595-603

HEMINGWAY B.S., H.T. EVANS Jr., G.L. NORD Jr., H.T. HASELTON Jr., R.A. ROBIE, J.J McGEE (1986) Akermanite: phase transitions in heat capacity and thermal expansion, and revised thermodynamic data. Canad. Mineral. 24, 425-434

HUGGINS F.E., H.K. MAO, D. VIRGO (1975) Mössbauer studies at high pressure using the diamond-anvil cell. Carnegie Institution of Washington, Year Book 74, 405-410

HUGGINS F.E., H.K. MAO, D. VIRGO (1976) Gillespite at high pressure: results of a detailed Mössbauer study. Carnegie Institution of Washington, Year Book 75, 756-758

INGALLS R. (1964) Electric-field gradient tensor in ferrous compounds. Phys. Rev. 133A, 787-795

JAGADEESH M.S., H.M. NAGARATHNA, P.A. MONTANO, M.S. SEEKRA (1981) Magnetic and Mössbauer studies of phase transitions and mixed valences in bornite ($Cu_{4.5}Fe_{1.2}S_{4.7}$). Physical Review B 23, 2350-2356

KIMATA M., N. II (1981) The crystal structure of synthetic akermanite, $Ca_2MgSi_2O_7$. Neues Jahrb. Mineralogie Monatsh. 1981, 1-10

LIEBAU F. (1983) Einteilung und Mechanismen von Phasenumwandlungen. Fortschr. Miner. 61, 29-84

LINARES J., J.R. REGNARD, N. VAN DANG (1983) Magnetic behaviour of grunerite from Mössbauer spectroscopy. J. Magnetism and Magnetic Materials 31-34, 715-716

LITTERST F.J., G. AMTHAUER (1984) Electron delocalization in ilvaite, a reinterpretation of its ^{57}Fe Mössbauer spectrum. Phys. Chem. Minerals 10, 250-255.

MADDOCK A.G. (1985) Mössbauer spectroscopy in mineral chemistry. In: Chemical Bonding and Spectroscopy in Mineral Chemistry (F.J. BERRY and D.J. VAUGHAN eds.), Chapman and Hall, London, 141-208

McCAMMON C.A., D.C. PRICE (1985) Mössbauer spectra of Fe_xO ($x > 0.95$). Phys. Chem. Minerals 11, 250-254

MÜLLER K.A. (1981) Paramagnetic point and pair defects in oxide perovskites. J. Physique 42, 551-557

MYSEN B.O., D. VIRGO (1985) Iron-bearing silicate melts: relations between pressure and redox equilibria. Phys. Chem. Mineral. 12, 191-200

NAVROTSKY A. (1980) Lower mantle phase transtions may generally have negative pressure-temperature slopes. Geophys. Res. Letters 7, 709-711

PARKIN K.M., B.M. LOEFFLER, R.G. BURNS (1977) Mössbauer spectra of kyanite, aquamarine, and cordierite showing intervalence charge transfer. Phys. Chem. Minerals 1, 301-311

PETERSEN J.F., M. AYDIN, J.M. KNUDSEN (1977) Mössbauer spectroscopy of an ordered phase (superstructure) of FeNi in an iron meteorite. Physics Letters 62A, 192-194

SAXENA S.K. (1983) Exsolution and Fe^{2+}-Mg order-disorder in pyroxenes. In: Kinetics and Equilibrium in Mineral Reactions, S.K. Saxena ed., 61-80, Springer-Verlag, New York

SAXENA S.K., S. GHOSE (1971) Mg^{2+}-Fe^{2+} order-disorder and the thermodynamics of the orthopyroxene crystalline solution. Am. Mineral. 56, 532-559

SEIFERT F.A. (1978) Equilibrium Mg-Fe^{2+} cation distribution in anthophyllite. Am. J. Sci. 278, 1323-1333

SEIFERT F.A. (1983) Mössbauer line broadening in aluminous orthopyroxenes: Evidence for next-nearest neighbours interactions and short-range order. N. Jb. Mineral. Abh. 148, 141-162

SEIFERT F.A., M. CZANK, B. SIMONS, W. SCHMAHL (1987) A commensurate-incommensurate phase transition in iron-bearing akermanites. Phys. Chem. Minerals. 14, 26-35

SEIFERT F.A., D. VIRGO (1975) Kinetics of the Fe^{2+}-Mg, order-disorder reaction in anthophyllites: Quantitative cooling rates. Science 188, 1107-1109

SIEGEL E., K.A. MÜLLER (1979) Local position of Fe^{3+} in ferroelectric $BaTiO_3$. Phys. Rev. B20, 3587-3595

SKOGBY H. (1987) Kinetics of intracrystalline order-disorder reactions in tremolite. Phys. Chem. Minerals 14, 521-526

TAYLOR M., G.E. BROWN (1976) High-temperature structural study of the $P2_1/a$ = A 2/a phase transition in synthetic titanite. Amer. Mineral. 61, 435-447

VIRGO D., S.S. HAFNER (1969) Fe^{2+}-Mg disorder in heated orthopyroxenes. Mineral. Soc. Amer. Special Paper 2, 67-81

WIVEL C., S. MÖRUP (1980) Improved computational procedure for evaluation of overlapping hyperfine field distributions in Mössbauer spectra. J. Phys. E14, 605-610

ZOU G.T., H.K. MAO, P.M. BELL, D. VIRGO (1980) High pressure experiments on the iron oxide wüstite. Carnegie Institution of Washington Year Book 79, 374-376

HIGH PRESSURE SPECTROSCOPY

K. Langer

Institut für Mineralogie und Kristallographie
Technische Universität, D1000 Berlin, Germany

The pressure acting on earth material increases by four orders of magnitude from the earth's surface down to the crust-mantle boundary and by six orders magnitude down to the mantle-core boundary. These changes exceed by far the concomitant temperature increase reaching only about one and a half or two orders of magnitude, respectively.

The enormous increase in pressure induces continuous and/or more or less discontinuous changes of the structure and the bonding properties and, as a consequence, of the physical and physicochemical properties of the mineralogical constituents of the above mentioned earth zones.

To understand such changes with pressure, diffraction experiments under pressure contributed a lot. On the other hand, questions of changes in electronic, vibronic, and thermodynamic properties, in radiation transmissivity, in transition metal bonding and partitioning behaviour and others can be solved only by spectroscopic methods adapted to high pressures.

High pressures in the above range can be experimentally realised in small volumes only, typically 0.005 mm^3. Therefore, only those spectroscopic methods can be adapted to high pressures which allow for small cross sections of radiation. Up to now, these methods are vibrational spectroscopy, i. e. IR-absorption and Raman scattering, X-ray absorption (XANES, EXAFS), ^{57}Fe γ-ray or Mössbauer resonance, and electronic resonance spectroscopy in the UV/VIS/NIR spectral ranges. The present paper discusses high pressure methods applied in the just mentioned spectroscopic techniques and some typical results, bearing on geoscientific problems. It is restricted to crystalline phases, mainly oxygen based minerals.

Typical problems in high pressure spectroscopy are (a) intensity of measuring radiation, which is mostly achieved by focusing techniques; (b) for static measurements, pressure resistant windows with high transparency in spectral ranges as wide as possible are required; (c) pressure distribution within and around the crystalline material under study has to be known and should be hydrostatic; simple methods of pressure measurements have to be available.

Most static measurements are performed using high pressure cells equipped with boron carbide windows in case of Mössbauer experiments, with diamond windows in case of X-ray absorption measurements, and with alkali halide or diamond windows in case of IR- and of UV/VIS/NIR-spectroscopy. Gasketing techniques are used to hold the embedding media, epoxy resin, alkali halides, alcohol mixtures, or perhalogenated paraffin oil. Two types of high pressure cells are used in static measurements, the Drickamer-type cell, with the pressure-generating force perpendicular to the measuring beam, and the opposed anvil type cell of Weir and coworkers, operating with force and beam in the same direction. Many modifications of the later, related to the experimental requirements, are in use. Pressure measurements are obtained by the shift with pressure of alkali halide X-ray diffraction lines, of absorption bands of nickel-dimethylglyoxime, or of ruby R_I-sharp line emission. In case of optical spectroscopy, there are also dynamic high pressure experiments by means of shock wave compression.

The highest pressures achieved so far in Mössbauer-resonance, X-ray emission, and in single crystal optical absorption in the UV/VIS/NIR ranges are near 20 GPa. In case of powder spectroscopy in the VIS to IR ranges, measurements have been performed up to 50 GPa, a pressure which was also obtained in optical absorption under shock wave compression.

High pressure EXAFS and XANES studies are useful for the determination of bond length and coordination number in unknown high-pressure phases, of local compressibilities around a specific atom in complex structures, and of the electronic structures of high pressure phases. By means of high pressure ^{57}Fe γ-ray resonance spectroscopy, changes with pressure of the geometry of Fe-sites in complex structures, changes with pressure of the electronic structure of Fe, as $Fe^{2+}Fe^{3+}$ charge transfer, pressure induced reduction of Fe^{3+}, or spin-pairing, as well as changes with pressureof the magnetic properties can be studies.

Vibrational spectroscopy, i. e. IR-absorption and Raman-scattering, under pressure records the shift with pressure of the internal and lattice vibrations in mineral structures, yielding e. g. the pressure dependence of hydrogen bonds and of microscopic Grüneisen-parameters.

When these are known for all structural units involved, then molar heat capacities, C_v, may be derived as a function of pressure. Including data on the temperature dependence of C_v, which may also be derived from vibrational spectra, enables to calculate the pT-dependence of phase transitions as shown in case of calcite/aragonite, andalusite/sillimanite, and others.

Optical high pressure spectroscopy has been performed between 250 (40000) and 2000 nm (5000 cm^{-1}), i. e. in the UV/VIS/NIR spectral ranges Theoretical evaluation of the observed changes with pressure of spectral absorption bands provides information about the pressure dependence of coordination geometry and electronic state of transition metal ions, M^{x+}, especially $3d^n$-ions. Pressure shifts of dd-transitions contribute to solve band assignments especially in case of spinforbidden transitions. Bands originating from dd-transitions and from intervalence charge-transfer transitions can be identified on the basis of their pressure behaviour. The pressure dependence of dd-bands allows for determining the change with pressure of crystal field splitting, 10Dq, and of Racah-parameter B, reflecting the interelectronic repulsion. From these data, pressure dependences of the crystal field stabilisation energy of M^{x+}, $CFSE_{M^{x+}}$, and estimations of change with pressure in the covalent character of the M^{x+}-O bond may be derived. Pressure dependence of $CFSE_{M^{n+}}$ yields information about partitioning behaviour of M^{n+} under varying pressure and about phase transformations. Local compressibilities of transition metal centered polyhedra may be determined from the pressure dependence of 10Dq. Inbetween the ranges of strong absorptionin the IR, by lattice vibrations, and in the UV, by electronic ligand-metal charge transfer, both allowed transitions in terms of selection rules, there exists a wavelength or energy range of relatively high transmission in silicate minerals. The pressure dependence of the energy width of this "optical window" is important in radiative heat transport and may be determined by high pressure spectroscopy.

MINERALOGICAL APPLICATIONS OF X-RAY ABSORPTION SPECTROSCOPY

Georges Calas, François Farges, Alain Manceau aand Jaqueline Petiau

Laboratoire de Minéralogie-Cristallographie, Universités de Paris 6 et 7 and CNRS, 75351 PARIS Cedex 05, France.

X-ray Absorption Spectroscopy (XAS) is one of the few element-specific methods, which can be applied to the determination of the local structure around a given element and provides also some chemical information concerning, e.g., its oxidation state or the nature of cation-ligand chemical bonding. This method has taken advantage of the high intensity, white beam character of synchrotron radiation, which explains its fast development in materials reasearch and more recently in Mineralogy. The mineralogical and geochemical applications of XAS encompass cation environments in complex solid solutions and poorly crystalline minerals, order-disorder relations, determination of oxidation states and bonding of elements in transition metal sulfides and oxides. It is also a choice method to investigate the formation media of the minerals, including silicate melts and glasses, aqueous solutions and gels.

XAS comprises two distinct regions referred to as X-ray Absorption Near Edge Structure (XANES), which extends up to some tens eV above the absorption edge, and Extended x-ray Absorption Fine Structure (EXAFS), which extends at higher energy over several hundreds eV. XANES comprises electronic transitions from core levels to the first empty bound states and multiple scattering resonances, where low energy photoelectrons are backscattered by the surrounding atoms. The general shape of the edge and the relative position and intensity of edge components provide information on oxidation state, coordination numbers and cation-ligand covalency, as well as site symmetry and actual structure of the first atomic shells around the absorbing cation. EXAFS oscillations derive from interferences between outgoing and backscattered photoelectrons, which can be modelled, in a first approximation, using a single-scattering, plane-wave formalism. The frequency of these oscillations depends on the absorber-scatterer distances and atomic phase shifts, and their amplitude is related to the number and backscattering efficiency of atoms surrounding the x-ray absorber, although disorder effects can severely alter the structural and chemical content of the information.

We will present a review of some recent results obtained on transition elements containing minerals (silicates, sulfides and oxides). The data obtained concern the actual distribution of elements in multisite minerals or the determination of oxidation states. Significant progresses concern the location of transition elements in supergene manganese oxides, the deviation from ideal behaviour of substituted minor transition elements in low-temperature phyllosilicates and the modification of the mineral structure by irradiation leading to the metamict state. The short range order and structural evolution of supergene ferric oxide gels during ageing and their evolution into crystalline iron oxyhydroxides will also be considered. XAS is also an efficient tool to determine the local structure of multicomponent glasses and has pointed out the specific paper played by the various components, as well as their contrasting behaviour during glass nucleation and crystallization. Finally, the recent technical improvements allow to study samples in conditions which are more relevant to their formation: high temperature is attained using a furnace on the XAS experiment and special devices are used to study melts and fluids; high pressure is obtained with various diamond-anvil devices; trace elements crystal chemistry is studied with fluorescence detection schemes and mineral surfaces with total electron yield detection; phase transformation kinetics may be followed with dispersive EXAFS which allows fast measurements. The advent of a new generation of storage rings such as the European Synchrotron Radiation Facility will greatly enhance the development of XAS in Earth Sciences.

Principles and potentials of XANES spectroscopy

Ivan Davoli

Dep. of Mathematic and Physics, University of Camerino, I-62032. Italy.

Extended Abstract.

The local structural distortions around the sites of impurities in dilute solid solutions were inferred from their effects on the intensities of diffraction peaks and from the associated diffuse scattering. With the availability of high intense sources (read Sychrotron Radiation Centers) spectroscopic techniques dealing with soft- and hard- X-ray absorption have been developed. Such techniques named EXAFS (Extended X-ray Absorption Fine Structure) and XANES (X-ray Absorption Near Edge Structure) provide a direct measurement around a selected atom giving information on structural order and on electronic properties.

The well established EXAFS spectroscopy has been used for a wide class of geochemical compounds, whether they occur as a trace or major elements in crystalline and/or in amorphous solids[1]. In the last decade, together with the massive use of the EXAFS, already supported by a theoretical background[2], a considerable effort was dedicated to the understanding of the XANES. Indeed, that the structures present in the first 50 - 60 eV were sensitive both to the electronic composition and to the geometrical arrangement around the excited atom was discovered late in the seventies[3], but a quantitative method comes only recently with the identification of the XANES as due to a multiple scattering resonances within a small atomic cluster of neighbor atoms[4]. The energy range of the XANES under this hypotesis is system-dependent and in some of the studied cases is extended from 10 up to the 150 eV. The first 8-10 eV is the so called "edge region" and may have different physical origin for different class of material[5]; bound valence states in molecules, transition to local empty states in metal or insulator and effects of many-body and multielectron configuration interactions.

In the XANES, like in EXAFS spectroscopy, the structural information are due to the scattering of the excited photoelectron with the neighboring atoms. In the EXAFS region the photoelectron is weakly backscattered by the neighbor atoms in a single-scattering process before coming back on the absorbing site and then escaping in the free space. This process gives information, only, about the pair distribution function. On the contrary, in the XANES region a multiple scattering process takes place; this makes the XANES spectra highly sensitive to the geometrical environment, and information beyond pair distribution function (angle between atomic bond) can be obtained.

The Multiple Scattering Theory (MST) is in the position to explain the features all over the absorption spectra starting from the Fermi golden-rule. The expression of the total absorption cross-section can be written as:

$$\sigma(\varepsilon) = 4\pi^2 \varepsilon \alpha \Sigma_f |\langle\psi_f|\underline{\varepsilon}\cdot\underline{D}|\psi_i\rangle|^2 \delta(\varepsilon - E_f + E_i) \qquad (1)$$

where the symbols have the usual meaning and are reported in ref.[7]. Many different approaches can be used to calculate the expression (1)[8], but each of them brings at the same numerical results. In our case we have used the Green function approach which is the most suitable to obtain structural information[9], so that the expression for the cross-section becames

$$\sigma(\varepsilon) = 4\pi\ (\varepsilon + I_0)\ \alpha\ K\ [\langle R_L{}^0|p\ D|\psi_{in}\rangle]^2\ \mathrm{Im}\ [(\underline{I} - T_a\ G)^{-1}\ T_a]_L{}^0{}_L{}^0$$

The absorption coefficient defined as $[\alpha(\varepsilon) = n\ \sigma(\varepsilon)]$ is given, for the cluster case[10], by:

$$\alpha_c(\varepsilon) = (l+1)\ \alpha_0{}^{l+1}(\varepsilon)\ \chi^{l+1}(\varepsilon) + l\ \alpha_0{}^{l-1}(\varepsilon)\ \chi^{l-1}\ (\varepsilon)$$

where $\alpha_0{}^l$ is the atomic absorption coefficient and

$$\chi^l(\varepsilon) = [1/(2l+1)][\ 1/\sin^2\delta_l{}^0]\ \Sigma_m\ \mathrm{Im}[(I - T_aG)^{-1}\ T_a]_{lm}{}^0{}_{lm}{}^0 \qquad (2)$$

is the factor which carries all the information about the environment. Under the hypothesis that the spectral radius of the matrix T_aG is less than 1, for the interest energy, an alternative way to write χ^l is:

$$\chi^l(\varepsilon) = 1 + [\Sigma_2\ \chi_n{}^l(\varepsilon)\ ]$$

and the term in the square parenthesis represents the partial contribution of order n. Those terms take in account for all the process in which the photoelectron emanating from the absorbing atom is scattered n-1 times by the surrounding atoms before returning to site 0 and then escaping in the free space. The orders of the scattering process are given by the letter n and, as is shown, can be infinite in principles. However because of the anelastic process the most important contributions are limited to the 3^{th} or 4^{th} scattering order from which we may deduce higher order distribution function. At low energy, where all the path are equaly important, only global information can be obtained, a relation between energy position of the continuum resonance and the bond length between the absorption atom and its nearest neighbors can be obtained. Following the procedure of ref. [8] we obtain:

$$(E_r - \underline{V})\ R^2 = C_r = \mathrm{cost.} \qquad (3)$$

where E_r is the energy position of the peak, R is the bond length between the absorbing atom and its first neighbors, in the real space, and $\underline{V}$ is an average interstitial potential peculiar of the particular cluster under investigation. In this expression the quantity $\underline{V}$ is not directly measurable; so to overcome this difficulty we subtract at the equation (3) a similar expression calculated for a pre-edge features due to transition to bound states like antibonding states of 3d character in the case of metal oxides [5].

$$(E_b - \underline{V})\ R^2 = C_b = \mathrm{cost.}$$

and the result of the subtraction gives:

$$(E_r - E_b)\ R^2 = \mathrm{cost.} \qquad (3)$$

where all the quantities are, now, experimentaly measurable.

Exploiting the relation (3) of the previous paragraph, we have studied Pyroxenes with different Ca concentration finding a distortion of the polyhedrom around the M2 site varying as a function of the Ca content[11]. The experiment was performed at the Frascati Synchrotron Radiation Center utilizing the "PULS X- ray line" [12] which use as monochromator a Si [111] single cut crystal and the spectra were detected in a trasmission mode utilizing two ionization chambers filled by a suitable gas

mixture.More recently, the quantitative method for the local structural determination was used in the study of another very important geochemical compound: the SiO_2. In two different samples, a pure quartz and a very densified vitreous silica, we have investigate the oxygen site structure by the XANES at the K edge of the oxygen (532 eV).

The spectra were detected at the "Grasshopper line"[13] of the mentioned laboratory using "partial yield technique". From the experimental data themselves, we could not say anything because the the paucity of the resolution, but with the help of the XANES simulation we note that the little red shift of the broad peak C (see Fig. 1) can be associated at the compression effect. In the simulation we have increased the oxygen bridging angle and we have had, as a correspondent effect, a light shift of the mentioned peak C to high energy. In this way we confirm the clue given by the experimental data.

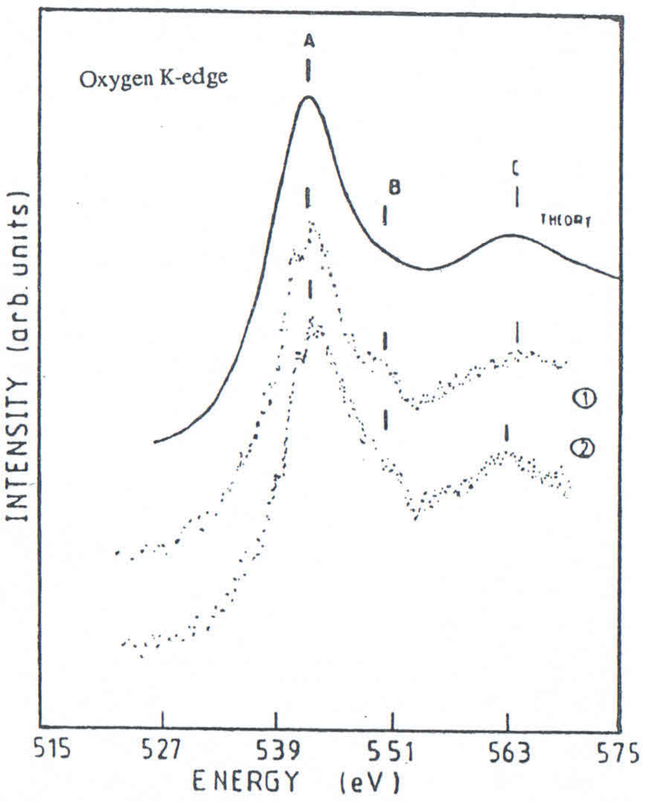

Fig. 1. Comparison of experimental and theoretical XANES. Upper curve is the calculated Oxygen K edge. Curve (1) and (2) are experimental data for the pure quartz and compressed SiO_2, respectively

REFERENCES

1. For a general review start from the Geochemistry section on: *"EXAFS and Near Edge Structure III"* Edt. by K.O. Hodgson, B. Hedman, and J.E. Penner-Hahn. Springer-Verlag. Berlin 1984.
2. D.E. Sayers, E.A. Stern, F.W. Lytle, *Phys. Rev. Lett.* **27**, 1204 (1971).
3. C.R. Natoli, D.K. Misemer, S. Doniach and F.W. Kutzler, *Phys. Rev. A* **22**, 1104 (1980). - F.W. Kutzler, C.R. Natoli, D. K. Misemer, S. Doniach and K.O. Hodgson, *J.Chem. Phys.* **73**, 3274 (1980). - A. Bianconi, S. Doniach and D. Lublin, *Chem. Phys. Lett.* **59**,121 (1978). - M. Belli, A. Scafati, A. Bianconi, S. Mobilio, L. Palladino, A. Reale and E. Burattini, *Solid State Commun.* **35**, 355 (1980).
4. C. R. Natoli. Frascati Report. INFN **LNF-87/83(PT) 1987**. - M. Benfatto, C.R. Natoli, A Bianconi, J. Garcia, A. Marcelli, M. Fanfoni, I. Davoli. *Phys. Rev. B* **34**, 5774 (1986). - C.R. Natoli, M. Benfatto. *Journal de Phys.* **47**, C8-11 (1986) and ref. therein.
5. A. Bianconi, *EXAFS for Inorganic System*, S.S. Hasnain and C. D. Garner (Eds). Daresbury Report **DL/SCI/R17 E**, 1981 p.13. - A. Bianconi, A. Giovannelli, I. Davoli, S. Stizza, L. Palladino, O. Gzowski, L. Murawski. *Solid State Commun.* **42**, 547 (1982).
6. A. Bianconi, M. Dell'Ariccia, A. Gargano, C.R. Natoli. *EXAFS and Near Edge Structure*. A. Bianconi, L. Incoccia, and S. Stipcich (Eds) Springer-Verlag Berlin 1983 p. 57.
7. Where $\psi_{i,f}$ are the initial and the final state wave functions, ε the photon energy, p the polarization versor, D the dipole transition operator and $\alpha = 1/137$ is the constant of fine structure.
8. C. R. Natoli. *EXAFS and Near Edge StructureIII* K. O. Hodgson B. Hedman, and J. E. Penner-Hahn (Eds). Springer - Verlag Berlin 1984 p. 38
9. P. J. Durham, J. B. Pendry C. H. Hodges. *Comput. Phys. Commun.* **25**, 193 (1982). - P. Lloyd, P. W. Smith. *Adv. Phys.* **21**, 69 (1972).
10. W. L. Schaich, *Phys. Rev.* **B29**, 6513 (1984).
11. I. Davoli, E. Paris, A. Mottana, A. Marcelli. *Phys. and Chem. of Minerals* **14**, 21(1987).
12. S. Mobilio, F. Comin , L. Incoccia INFN **LNF-82/19(NT)** 1982.
13. P. Chiaradia, M. Fanfoni, S. Priori, P. De Padova, P. Nataletti, I. Davoli, S. Modesti *Vuoto* **16**, 83 (1986).

UNIVERSITA' " LA SAPIENZA " CENTRO STAMPA D'ATENEO
ROMA Piazzale Aldo Moro , 5 - settembre 1988